



Article

Application of Radar-Based Precipitation Data Improves the Effectiveness of Urban Inundation Forecasting

Doan Quang Tri ^{1,*}, Nguyen Vinh Thu ², Bui Thi Khanh Hoa ², Hoang Anh Nguyen-Thi ², Vo Van Hoa ³, Le Thi Hue ³, Dao Tien Dat ³ and Ha T. T. Pham ⁴

¹ Journal of Hydro-Meteorology, Information and Data Center, Viet Nam Meteorological and Hydrological Administration, Hanoi 10000, Vietnam

² National Centre for Hydro-Meteorological Network, Viet Nam Meteorological and Hydrological Administration, Hanoi 10000, Vietnam; nvthu@monre.gov.vn (N.V.T.); khanhhoa303@gmail.com (B.T.K.H.); hoanganhck@gmail.com (H.A.N.-T.)

³ Northern Delta and Midland Regional Hydro-Meteorological Center, Viet Nam Meteorological and Hydrological Administration, Hanoi 10000, Vietnam; vovanhoa80@yahoo.com (V.V.H.); minhhuekttv@gmail.com (L.T.H.); daodat81@gmail.com (D.T.D.)

⁴ Faculty of Environmental Sciences, University of Science, Vietnam National University, Hanoi 10000, Vietnam; phamthithuha.hus@gmail.com

* Correspondence: doanquangtrikttv@gmail.com; Tel.: +84-98-892-8471



Citation: Tri, D.Q.; Thu, N.V.; Hoa, B.T.K.; Nguyen-Thi, H.A.; Hoa, V.V.; Hue, L.T.; Dat, D.T.; Pham, H.T.T. Application of Radar-Based Precipitation Data Improves the Effectiveness of Urban Inundation Forecasting. *Sustainability* **2024**, *16*, 3736. <https://doi.org/10.3390/su16093736>

Academic Editor: Magnus Moglia

Received: 4 April 2024

Revised: 25 April 2024

Accepted: 28 April 2024

Published: 29 April 2024



Copyright: © 2024 by the authors. Licensee MDPI, Basel, Switzerland. This article is an open access article distributed under the terms and conditions of the Creative Commons Attribution (CC BY) license (<https://creativecommons.org/licenses/by/4.0/>).

1. Introduction

Weather radar and rain gauges are both devices used to monitor rainfall, and these rainfall data sources can be employed as inputs for hydrological models [1–3]. Rain gauges provide the accuracy of point measurements and are often considered ground truth [4,5], although they also have potential errors, such as random or systematic errors [6,7]. Previously, the selection of parameter sets for hydrological models was based mainly on rain gauge stations [8,9]. However, the disadvantage of these point measurements is that they

have low spatial resolution, owing to their dependence on the density of rain gauges, especially in high mountainous areas, coastal areas, and areas with complex terrain. Meanwhile, weather radar can estimate precipitation continuously over space and time [10], including areas with sparse rain gauge networks. This has been helpful in filling the gaps in rainfall monitoring in these areas. Quantitative precipitation estimation (QPE) often contains errors in the measurement process and the conversion of reflectivity to precipitation intensity [5]. Therefore, although QPE produces continuous, real-time rainfall data, the internal errors associated with radar measurements are the reason its use is limited in flood forecasting [11]. Two ways to improve QPE results involve the dual-polarization approach or adjusting the values to obtain a match between radar and the rain gauge [12–14]. In Vietnam, because there are no disdrometer devices, simulating the variation in particle size distribution to calculate the QPE from dual-polarization variables is difficult, so the data fusion approach is used. Radar and rain gauge data are the most suitable. A significant improvement in QPE has been observed in recent years in Vietnam [15,16]. Kimpara et al. [17] presented the use of the QPE method in applying the algorithms of the Japan Meteorological Agency [18] in Vietnam. They combined this with the development of improved techniques related to building clutter maps for each radar, adjusting the composition table of the lowest elevation angles to consider the influence of side-lobe radar beams, increasing the QPE data update time to every 10 min, etc. Kimpara et al. [15] contributed to minimizing the errors caused in the process of creating radar-based precipitation and enhancing QPE quality in Vietnam.

Forecasting the possibility of flooding in urban areas in a short period is a great challenge for scientists because of the complex relationships between meteorological systems or the simulation of the microphysical processes when incorporated into hydrological models. The accuracy of flood forecasts in general and urban flooding forecasts in particular depends on the ability to predict rainfall, flow, etc. If the quantitative precipitation forecasting (QPF) results are not accurate, they will lead to results in streamflow forecasts that are limited [19,20], owing to the uncertainties related to the hydrological model structure, parameterizations, and initial conditions of the stream model [21,22]. As the forecast horizon increases, the QPF results often tend to decrease [23], so it is necessary to carefully consider the application of long-term QPF in streamflow forecasting. In recent years, QPF techniques using radar data, including optical flow [24–26], VET of MAPPLE [27,28], and TREC [29,30], have received increasing research attention. With strengths in tracking continuously moving objects over a range of short periods, the optical flow technique has been applied in QPF. It has been proven to be one of the most effective techniques for extremely short-term rainfall forecasting and is currently being used in Vietnam [31]. Flood forecasting for rivers and streams often uses QPE instead of QPF because QPF has more potential than QPE [32]. However, this is only the case when there is rainfall that the QPE is created, so hydrological forecasts cannot be made until the rainfall event has occurred, and the full impact of the phenomenon cannot be captured in the streamflow forecast until the rain ends. This often occurs in small river basins where rainfall may not have ended before flash flooding begins. Therefore, the flexible use of QPE or QPF as hydrological model input should be tested to evaluate the feasibility of simulating flood events, flash floods, and urban inundation based on QPE and QPF calculated from radar.

In the world to date, there have been many studies applying different models to simulate urban flooding, and one of these is the MIKE URBAN model. One of these studies by Mark et al. [33] developed a flood model using MIKE URBAN in Central Dhaka, where the model simulated the rainfall–runoff process. The urban drainage network was computed using MIKE FLOOD, while the surface flow was calculated using a 2D model with a 10 m grid size. The model calibrated the water levels in the urban rivers for the flood and compared them with the prepared flood map, revealing a good agreement between the detected and simulated flood zones. Chen et al. [34] used the MIKE URBAN model to simulate urban flooding in Eastern and Central Dhaka. The MOUSE and MIKE FLOOD models simulated storm sewer and river channel flows. The rainfall and water levels in the rivers for flood modeling were calculated based on a statistical analysis of 50 years

of historical data from Dhaka's catchments. Luan et al. [35] successfully constructed the MIKE URBAN model in Lincheng city, China. The situation regarding the waterlogging of different surface runoff processes and the running state of the drainage pipeline network in the study area were illuminated. The simulated results showed that the water logging pressure in the typical mountain region and the old town was greater than that of the plain region and the new area. With the increase in the return period, the accumulated flow, the pressured pipeline number, and the overflow node number increase accordingly. The related analysis provides technical support for the early warning of urban waterlogging and the construction of drainage infrastructures in the study area and provides references for the simulation of the surface runoff process in mountainous cities. Yin et al. [36] used the MIKE URBAN model to establish the drainage model of a pipeline network to simulate the drainage situation when faced with different river water levels at the outlet. The results analyzed the relationship between pipe network drainage and the river drainage recurrence period considering the river storage capacity. Olsson [37] simulated water flow using the MIKE URBAN model based on X-band radar data. The study compared simulation results from the model with input rain data from measuring stations and input rain data from X-band radar, evaluating the effectiveness of using X-band radar data to improve the accuracy of flow simulation.

In Vietnam, recent studies have applied the MIKE URBAN model to calculate and simulate flood and urban inundation. Dung [38] applied the MIKE URBAN model to evaluate the impact of climate change on flooding in Hanoi city. The set of model parameters was calibrated and validated with the rainfall events in 2012 and 2013. The model was then used to calculate flooding in Hanoi with rainfall frequencies of 10% and 1%, with the results provided in flooding maps. Binh et al. [39] applied the MIKE URBAN model to calculate the water supply network for Tam Ky city, Quang Nam–Da Nang, according to the 2030 orientation plan. Doan et al. [40] evaluated the impacts of an improved sewer system in city flood inundations using the MIKE URBAN model. The model was calibrated and validated at three typical sites for the data on 16 October 2021 and 7 November 2021 and evaluated for the heavy rain data on 14 October 2022, and scenarios were tested for 2030. Hung and Lien [41] applied an urban hydrology model and green design for the drainage system of Ha Tinh city. Three scenarios were calibrated and validated to confirm the correctness and practical ability of the urban hydrological model. In the context of climate change, the scenarios showed that without timely measures, the drainage system will be overloaded, even for low-emission RCP4.5 scenarios. In addition, two proposals with a green design approach showed that it is feasible to reduce floods at a low cost and sustainably. Dai et al. [42] built an urban flood forecasting system for the Hanoi area using high-resolution grid rain data. The study results built a real-time urban flood forecasting system using $1\text{ km} \times 1\text{ km}$ high-resolution grid rain data from the weather research and forecasting (WRF) model for eight urban districts in Hanoi.

Recently, each time it has rained heavily in Nam Dinh city, the inundation has increased, significantly affecting people's daily lives and trade [43]. These heavy rains continued for long periods, resulting in insufficient time for Nam Dinh city's sewer system to drain the water. In addition to the weather factor, heavy rainfall and floods make water drainage difficult. Statistics reveal that rainfall lasting 30 consecutive minutes results in roads showing signs of inundation at the top of the road and sequentially. The lowest locations in the city will be the areas that experience the earliest and longest flooding. Flooding occurs not only with heavy rains of over 100 mm but also with moderate rains of 50–60 mm falling in a short period [44]. This situation is also relatively serious. Therefore, urban flooding causes heavy damage to motorbikes and other vehicles, and it has a great impact on the economy, traffic, and people's livelihood. There have been some flood and inundation studies conducted in Nam Dinh city, but they have stopped at the level of studying urban flooding and future flooding under climate change scenarios [45,46]. Nam Dinh province does not have any tools or models to support forecasters in urban flooding forecasting. In recent years, owing to unusual changes in weather, there have

been many prolonged heavy rain periods, precipitation exceeding the design frequency, and precipitation exceeding historical levels; thus, Nam Dinh city has continuously faced widespread flooding. Forecasters have not calculated all the possible scenarios. Therefore, a flood warning system that is triggered by heavy rain based on the radar-based precipitation forecast approach for Nam Dinh city is necessary. This study uses the rainfall from radar (QPE/QPF) as input to the MIKE URBAN model to simulate and forecast inundation and flooding for Nam Dinh city areas. The effectiveness of precipitation from radar will improve the accuracy of urban inundation simulation results, especially in Vietnam where urban floods occur quite frequently in large cities.

This study's objectives are as follows: (1) calculate QPE and QPF from radar for Nam Dinh province, (2) compare and evaluate the simulation results with precipitation radar and rain gauge data from a hydro-meteorological station for the Nam Dinh city area, (3) set up, calibrate, and validate the MIKE URBAN model, and (4) evaluate the effectiveness of urban inundation forecasting.

2. Materials and Methods

2.1. Description of the Study Area

Nam Dinh city is located at $106^{\circ}12'$ east, $20^{\circ}24'$ north, approximately 90 km from Hanoi, about 80 km from Hai Phong, 28 km from Ninh Binh, and 45 km from the east coast. The city is close to the growth triangle Nam Dinh–Hai Phong–Quang Ninh. Located in the center of the Northern Delta, Nam Dinh city has a national transportation network consisting of convenient rail, road, and waterway systems. Nam Dinh city is situated in the north of Nam Dinh province, the north and northeast border of Thai Binh province, the northwest borders of My Loc district, the southwest borders of Vu Ban district, and the southeast borders of Nam Truc district (Figure 1).

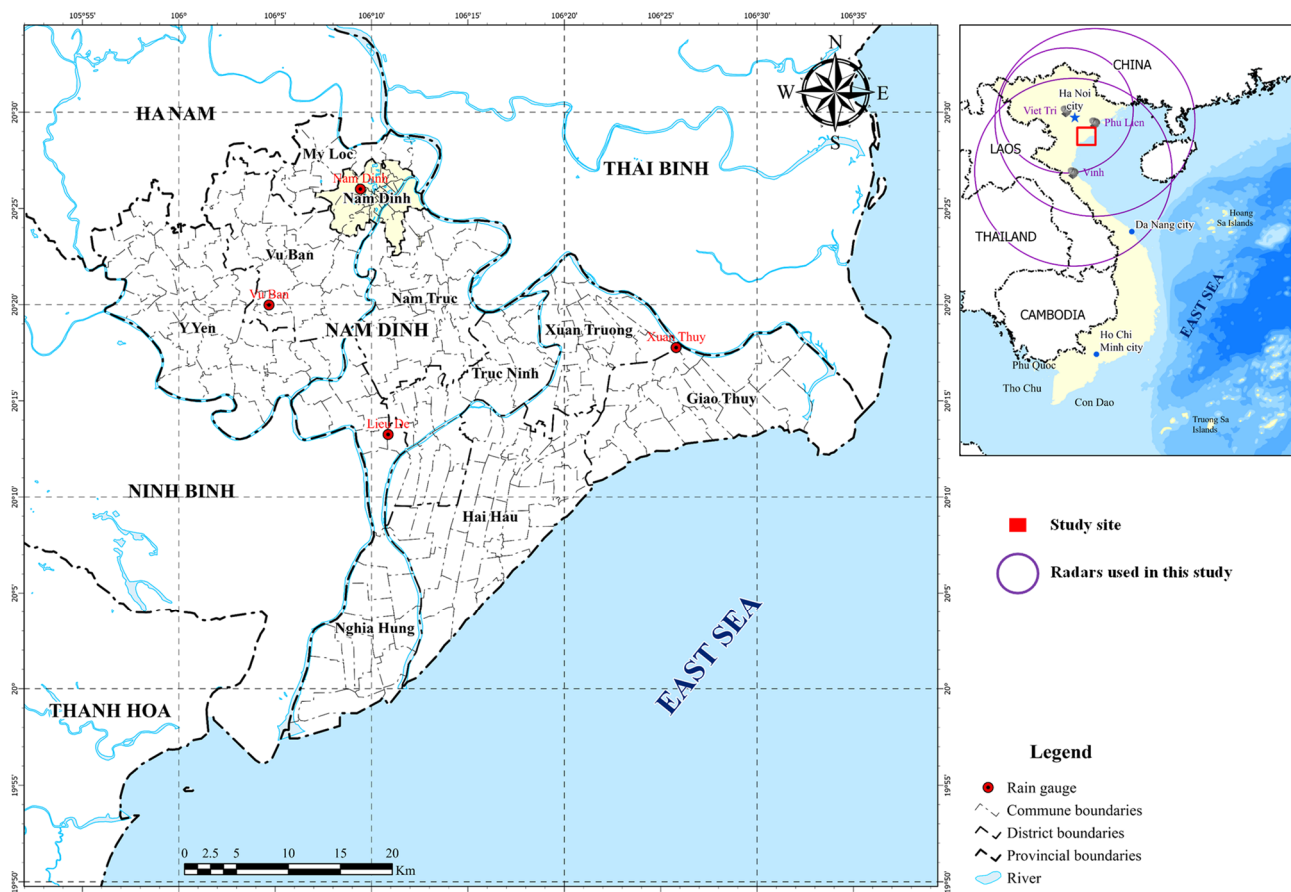


Figure 1. Study location map.

Nam Dinh city center currently uses a common drainage system. Rainwater and wastewater in this area are concentrated in underground sewers that flow in the opposite direction to the natural terrain (from east to west) and then into the drainage canal system in the area. Suburban areas mainly drain naturally according to the topography, and the water concentrates in the natural canal system in the area or through the existing sewer system, forced by pumping stations to the Red River and the canal. The Nam Dinh city center drainage system has a mixed structure, including 48.5 km of reinforced concrete sewer lines ranging in size from 300 to 2000 m, 22 km of open ditches (built ditches and dirt ditches), and 60 hectares of lakes and ponds, namely, Vy Xuyen, Vy Hoang, Truyen Thong, Son Nam, An Trach, Bao Boi, Nang Tinh, Do lagoon, Loc Vuong, and Hang Nan. The central drainage system of Nam Dinh city is divided into three main drainage basins: northeast, southwest, and northwest. Although the city's current network is basically perfect, it still does not meet the requirements for separating rainwater and wastewater. When there is heavy rainfall, rainwater cannot drain because of inadequate sewer sizes, so some areas become inundated. Statistics show that in recent times, the level of urban flooding has increased: 8 flooded points in 2015 to 18 points in 2017 (flooding time is 20–25 h with an inundation depth of approximately 30–100 cm).

To compare and evaluate the QPE and QPF results in Nam Dinh province, this study interpolated rainfall values to four automatic rain gauges, namely, Xuan Thuy, Lieu De, Vu Ban, and Nam Dinh with station codes 43546, 771429, 792845, and 48823, respectively. The distribution of the four observation points is shown in Figure 1. The QPE/QPF combination data of the three radars, Viet Tri, Phu Lien, and Vinh, were extracted to the location of the four rain gauges mentioned above (Figure 1).

2.2. Methodology

The study structure is presented in Figure 2. Input data for the inundation simulation model are QPE, QPF, and observed rain gauge. A MOUSE model is used to simulate the drainage system of Nam Dinh city. A couple of MOUSE-2D models in the MIKE URBAN model are used to calculate and determine inundation depth (Figure 2).

2.2.1. Description of the Method for QPE and QPF

QPE data are often used in urban flood forecasting because they provide information about the high spatial and temporal distribution of precipitation. This study used data from two S-band radars in Phu Lien and Vinh and one C-band radar in Viet Tri. The locations of the three radar sites are shown in Figure 1. The QPE method using these radar data is an improved method based on the original by Makihara [18]. First, these radar data need to be quality controlled (using clutter maps and quality control algorithms from the Finnish Meteorological Research Institute (<https://github.com/fmidev/rack> (accessed on 20 February 2024))), and then converted to rainfall intensity using the Marshall–Palmer relationship every 10 min. They are then combined with data from a rain gauge to correct the rainfall intensity data converted from the original Marshall–Palmer formula to obtain the cumulative rainfall accumulated over one hour as closely as possible to the actual rainfall through the two-step calibration. That is, the entire observing range of the three radars mentioned above is calibrated with a fixed coefficient in the first calibration, and for the second adjustment, each rain gauge site is calibrated and accompanied by a weight. Finally, a map of one hour's cumulative precipitation composition is produced. For the first calibration, it is necessary to ensure that the radar reflectivity intensity on a certain grid area is equal to the average value of all the other radars that monitor on the same grid, and the average value of the calibrated echo return strength on a given grid must be equal to the average value of the rain gauges. The second correction allows for a more detailed representation of precipitation distribution on a local scale. This study uses rain gauge stations within 1 km × 1 km grid cells around the station point to calibrate using weighted interpolation. The correction factor is defined as the ratio between the observed value of the rain gauge and the accumulated first corrected echo intensity. Factors taken

into account during the weighting of the interpolation include the distance between the grid cell and the rain gauge, the difference between the reflectivity return strength at the grid point and the rain gauge, the rate of attenuation of the radar beam to the amount of precipitation, and the distribution density of the rain gauge. Thus, the QPE data are the cumulative rainfall data per hour, updated every 10 min. This two-step calibration method was presented in Makihara [18], with the parameters adjusted in this study to suit the Vietnamese conditions. Detailed improvements were shown by Kimpara et al. [15]. The method of calculating QPF from radar uses the optical flow technique with a set of adjustable parameters, such as the ROVER_VN model described by Thu et al. [31]. QPF precipitation is also updated continuously every 10 min.

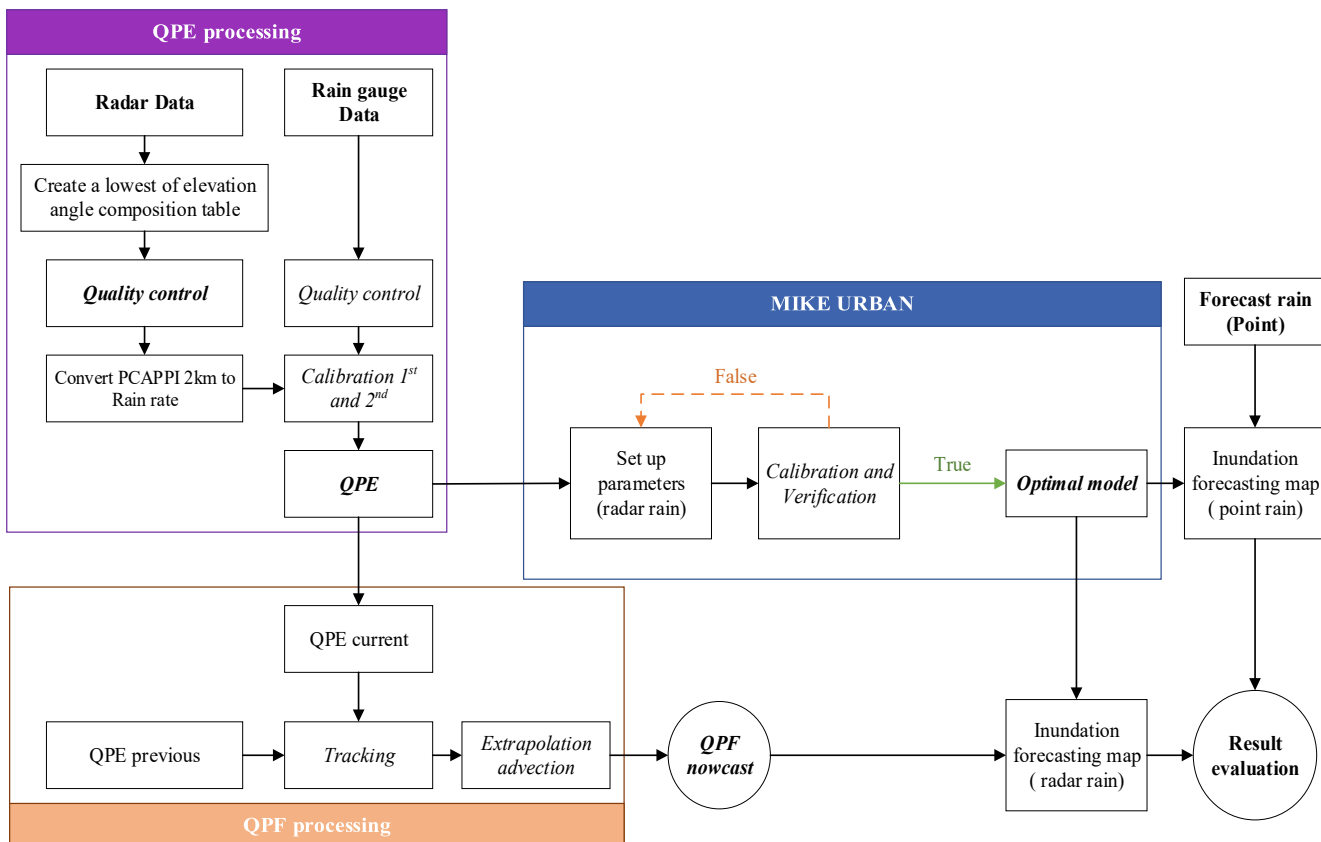


Figure 2. The flowchart of the study structure.

To compare and evaluate the results of QPE and QPF in Nam Dinh province, this study interpolated rainfall values to four automatic rain gauges, namely, Xuan Thuy, Lieu De, Vu Ban, and Nam Dinh with station codes 43546, 771429, 792845, and 48823, respectively. The observing frequency of Nam Dinh station (code 48823) is every hour, so data from this station do not participate in the radar rain gauge calibration process according to the QPE method proposed above. The distribution of four observation points is shown in Figure 1. The QPE/QPF combination data of three radars, Viet Tri, Phu Lien, and Vinh, were extracted to the location of the four rain gauges mentioned above. The station interpolation method is performed by taking the largest value of nine neighboring grid cells from around the considered station location.

2.2.2. Description of Models

The MIKE URBAN model is a flexible system for modeling and designing water distribution networks and collection systems for wastewater and stormwater. The MIKE URBAN model is based on a database for the storing network as well as hydraulic modeling data. This database is based on the Environmental Systems Research Institute (ESRI)

geodatabase. The geodatabase is a structure on top of a normal relational database, meaning that the underlying technology can be based on any of the major database vendors (Microsoft, Oracle, IBM, etc.). The geodatabase is the native storage structure for geographic information systems (GIS) data and may also be operated directly by standard GIS applications [47]. The modular structure of the MIKE URBAN is presented in Figure 3. The core module, MIKE URBAN, contains the possibility of modeling both water distribution and collection systems.

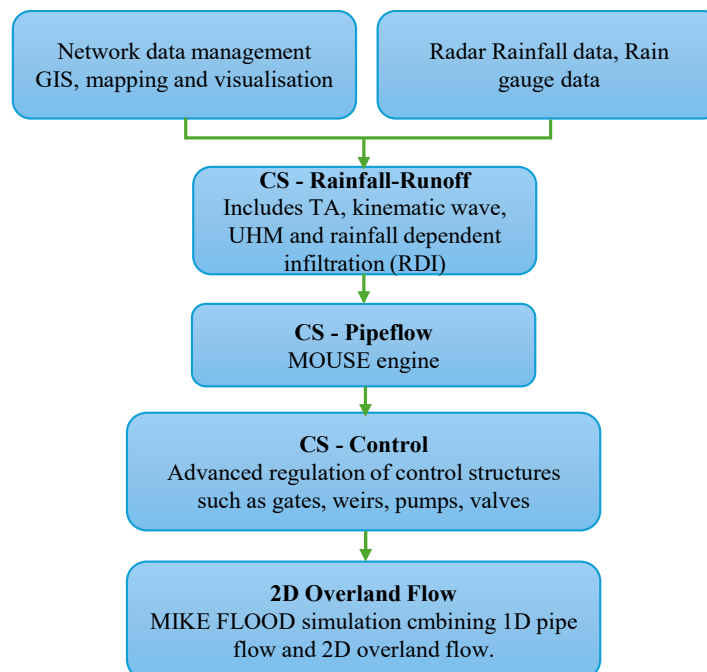


Figure 3. The modular structure of MIKE URBAN.

This study uses the following modules: collection system (CS) rainfall-runoff; CS PipeFlow, and two-dimensional (2D) overland flow. CS rainfall-runoff simulates the process of runoff from rain in the area. The output from this module is used as input for CS PipeFlow, simulating the flow process generated from rain through the drainage system in the study area. CS control is considered capable of operating the real-time monitoring of spillways, outlets, pumps, etc. It allows the description of control device operations and provides clear logic on the operating mode. After simulating the flow regime in the public system, 2D overland flow is used to simulate the process of water overflow from manholes to the study area terrain. Below is a detailed introduction of the modules used.

a. CS rainfall-runoff

The rainfall-runoff model consists of catchments connected to the hydraulic network through catchment connections. The rainfall-runoff model calculates runoff hydrology from an input rain data series. The hydrological model has several methods, namely, the area-time method, the kinematic wave method, the linear reservoir method, the infiltration-dependent rainfall calculation method, and the hydrological unit method.

The area-time method is a conceptual model used for calculating runoff in which the area contributing to the surface runoff increases with time according to a defined area-time curve. Several parameters need to be determined for each model catchment impervious area, such as water concentration time, area-time curve, hydrological reduction coefficient, and initial loss. The impervious area parameter determines the impermeable fraction for the model catchments. Only impermeable parts of the catchment are considered to contribute to surface runoff (Figure 4).

Water concentration time describes the time required for a water droplet to travel from the furthest part of the catchment to the catchment's outlet. The area-time curve describes

how the proportion of catchment area contributing to surface runoff increases over time. The hydrological reduction coefficient describes the extent to which a fraction of the input rainfall will be converted into runoff. Initial loss is the volume of water required to initiate surface runoff.

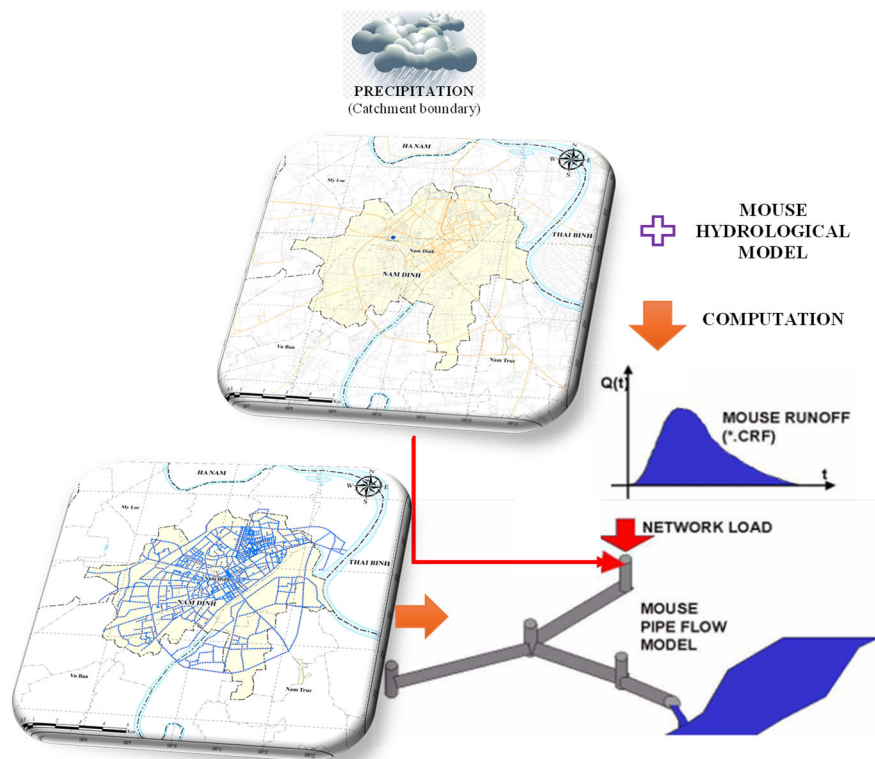


Figure 4. Illustrated flow of information in hydrological modeling.

b. CS PipeFlow

The MOUSE hydraulic and drainage network model is a one-dimension (1D) unsteady flow simulation tool. The 1D Saint-Venant equation is solved using the finite difference method. The network model consists of nodes connected through links. Network simulations are performed using the output from a rainfall runoff simulation model as input for flow calculations in the drainage network.

Link: The link in the MIKE URBAN model describes a pipe or channel in a water collection system. A link is characterized by its up- and down-level nodes, material, and size. The control nodes determine the length and slope of the link. The choice of material will affect the friction parameters in the connection. The size of a pipe is determined by the pipe diameter. For open channels, a cross-section describing how width changes with depth must be determined.

Nodes and constructions: Model links are connected to each other by nodes. Manholes, basins, weirs, pumps, and other structures are depicted as nodes in the MIKE URBAN model. Manholes are characterized by ground elevation, bottom elevation, and diameter. The head loss in manholes can be calculated using the Engelund formula or can be assumed to be zero using the “Do not change cross-section” option. Ponds, wetlands, marshes, and other storage elements are modeled as catchments in the MIKE URBAN model. A catchment is defined by base elevation, top elevation, and catchment shape. The catchment shape describes how the storage volume increases with the water level in the catchment. Dams are modeled as connections between two nodes. Overtopping a dam can be calculated using the weir formula or a user-defined table that determines the overtopping discharge for a series of water levels above the weir crest.

c. CS control

The “CS-control” module serves for the regulation and modification of control structures, like pumps and weirs, from a sewer system. During a simulation, it is possible to intervene with the control structures. In the end, the “2D overland flow” module is a major and important part of an urban flood simulation. This module enables MIKE URBAN to use a MIKE FLOOD simulation in the scope of the software. Thus, it is not necessary to use these software packages separately [48].

d. Two-dimensional overland flow

Surface flooding can be simulated with MIKE URBAN using the following two approaches.

- Combined 1D and 2D model: The flow in the subsurface pipes is simulated using the MOUSE 1D engine, and the overland flow is simulated using the MIKE 21 2D overland flow model. This combination of models is called MIKE FLOOD. The main input required for the 2D overland flow model is a digital elevation model. Based on this, the 2D model can simulate overland flow paths and velocities.

The main advantages of using this approach are that it leads to more reliable and more accurate modeling, requires less engineering judgment, requires fewer engineering hours, and provides better result visualization.

- Two-layer 1D model: The flow in the subsurface pipes as well as the overland flow are both simulated using the MOUSE 1D engine in MIKE URBAN. This approach requires that the overland flow paths (streets, etc.) are known or estimated beforehand, and each flow path is then defined as an open channel in MIKE URBAN. The flow exchange between the pipes and the overland channels is accounted for using the MIKE URBAN model components, such as weirs, orifices, or curb inlets. The engineering time and judgment required to predefine the overland flow paths can be substantial, and this is one of the main disadvantages of this approach. It also adds uncertainties and inaccuracies to the modeling since the model will only allow the overland flow to take place along paths anticipated by the modeler.

This study uses a combined 1D–2D model to simulate the inundation in the study area.

Data Collection

(a) Observed and estimated/forecasted rainfall

There are various techniques available to measure precipitation. Rain gauges have been used and developed for centuries, and today, a variety of models and techniques are used, both with manual and automatic operation [49]. Different types of radars for weather observation and measurements were first used in the 1940s, and there have been major developments since then [50]. These days, radar may also be used to estimate precipitation [51].

Data from automatic rain gauge stations, such as Xuan Thuy, Vu Ban, and Lieu De, are used to calibrate radar rainfall intensity after applying the Marshall–Palmer formula to convert reflectivity intensity to precipitation intensity. Data from these three sites and the Nam Dinh hydro-meteorological station are used to evaluate the results of QPE and QPF calculations from radar. Specifically, rainfall data from the Nam Dinh hydro-meteorological site were used as input data for the MIKE URBAN model, and the information related to water depth was used to evaluate the accuracy of the urban flooding scenario simulation results.

This study used three periods of heavy rain causing urban flooding in Nam Dinh city as follows:

- Event 1: the rainfall period from 10:00 UTC on 13 October 2020 to 09:00 UTC on 15 October 2020 (Event 1);
- Event 2: the rainfall period from 00:00 UTC on 8 September 2021 to 00:00 UTC on 9 September 2021 (Event 2);

- Event 3: the rainfall period from 21:00 UTC on 11 August 2022 to 07:00 UTC on 12 August 2022.

The QPE values of the first two rainfall events were used to determine the optimal set of parameters to include in the MIKE FLOOD simulation model. QPF radar data were included in the inundation forecasting models. Then, a comparison was made between a flood simulation model using QPF radar as input and a flood simulation model using station rainfall as input.

Radar rainfall data were extracted from grid type to point using the interpolation method to take the maximum value in the area of nine grid cells around the site location. The evaluation results of the quality of the rainfall data are shown in Section 3.

(b) Manhole and sewer system data in the study area

Information regarding Nam Dinh city's sewer and manhole system was collected from a status diagram of Nam Dinh city's rainwater and wastewater drainage system in the Nam Dinh city planning for 2030, vision to 2050.

(c) Topographical documents

A digital elevation model (DEM) of Nam Dinh city was collected from the Department of Survey and Mapping Vietnam (Figure 5).

Cross-sectional data of major rivers in the study area were collected from projects that were implemented in Nam Dinh city.

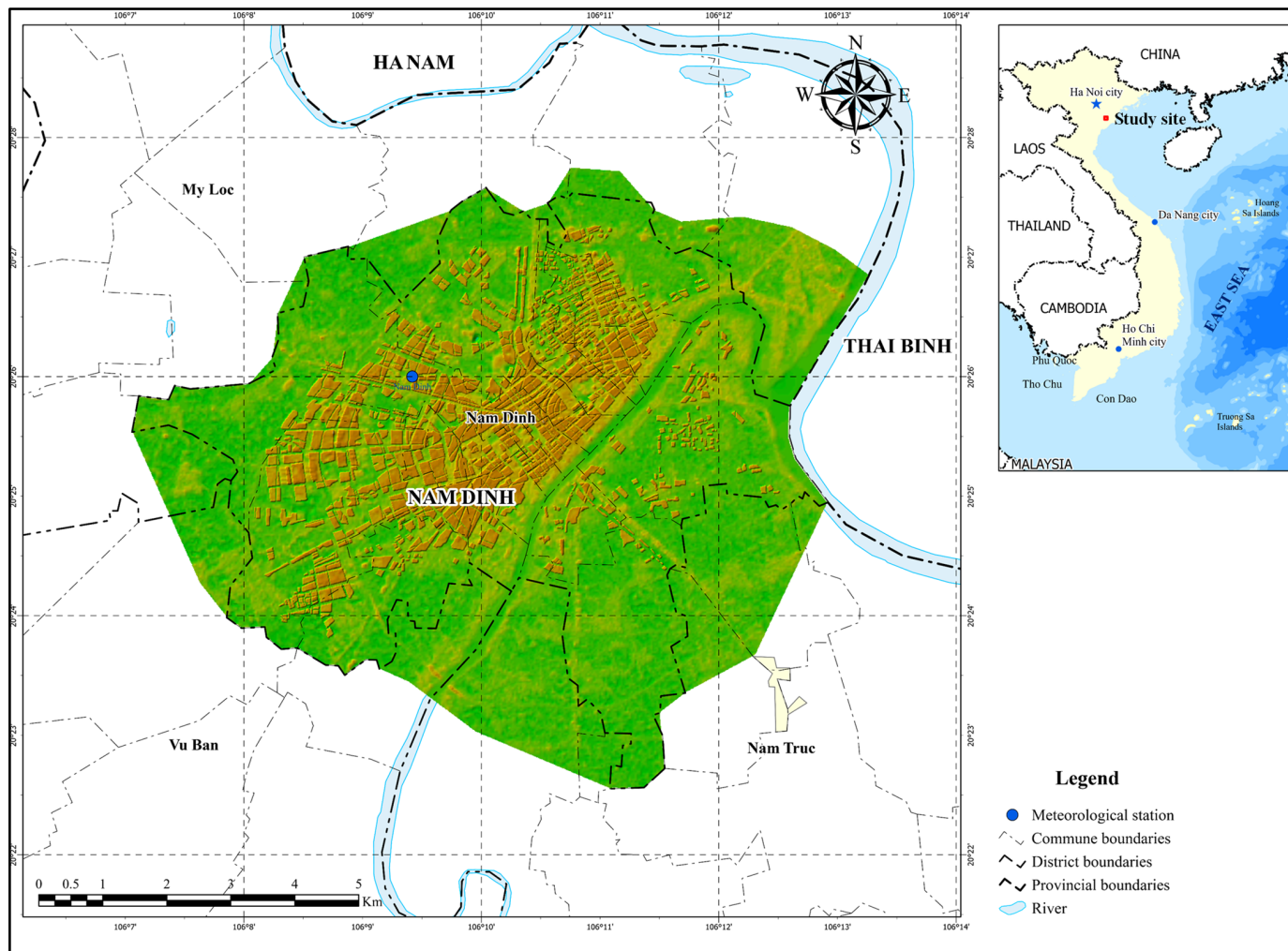


Figure 5. DEM of Nam Dinh city.

(d) Inundation survey location

This study investigated Nam Dinh city to collect inundation data on certain roads from the first two rainfall events (Event 1 and Event 2), which were used to calibrate and validate the model (Figure 6 and Table 1).

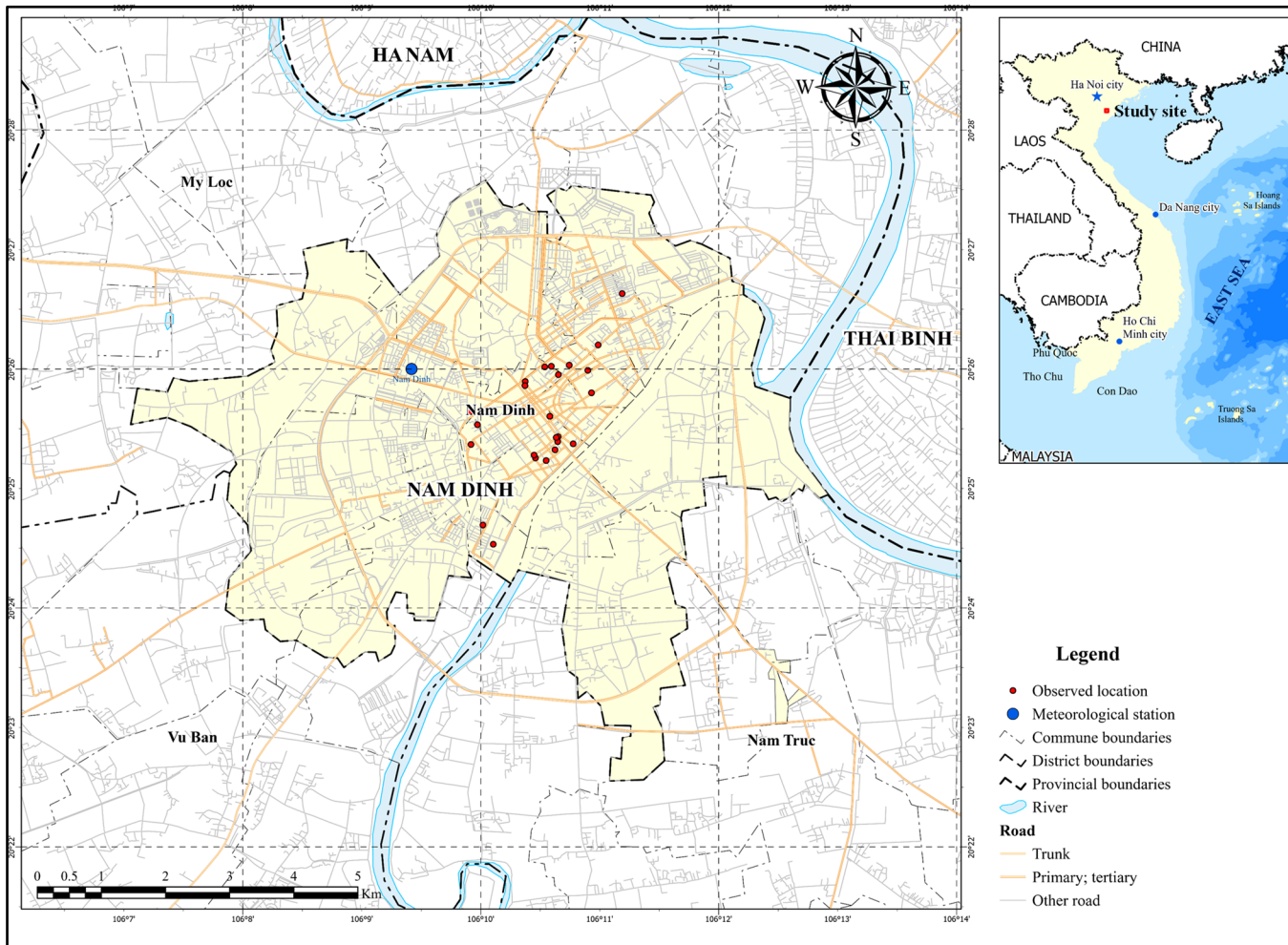


Figure 6. Inundation survey location map.

Table 1. Inundation survey locations.

No.	Location	Latitude (°N)	Longitude (°E)	Event 1 (m)	Event 2 (m)	Event 3 (m)
1	Vi Hoang	20.434	106.179	0.3–0.5	0.2–0.3	0.2–0.4
2	Nguyen Du	20.433	106.182	0.4–0.6	0.2–0.4	0.3–0.5
3	Tran Hung Dao	20.432	106.173	0.5–1.0	0.4–0.6	0.5–0.8
4	Ly Thuong Kiet	20.431	106.173	0.4–0.6	0.2–0.4	0.3–0.5
5	Luong Van Can	20.444	106.186	0.2–0.4	0.1–0.3	0.1–0.4
6	Luong The Vinh	20.427	106.165	0.2	0.1	0.2
7	Doan Tran Nghiep	20.426	106.166	0.2–0.5	0.2–0.3	0.2–0.4
8	Tran Dang Ninh	20.423	106.165	0.5	0.2–0.3	0.4
9	Tran Binh San	20.412	106.167	0.3–0.5	0.2–0.3	0.3–0.4
10	Han Thuyen	20.437	106.183	0.6–0.7	0.3–0.5	0.5–0.6
11	Le Hong Son	20.427	106.168	0.2–0.5	0.1–0.35	0.2–0.45
12	Le Hong Phong	20.43	106.182	0.4	0.2	0.2–0.3
13	Tran Quang Khai	20.409	106.168	0.2–0.5	0.15–0.3	0.2–0.4
14	Cau Do Quan	20.424	106.178	0.3–0.4	0.2–0.3	0.3–0.4
15	Hang Thao	20.423	106.177	0.6–0.7	0.3–0.5	0.4–0.6

Table 1. Cont.

No.	Location	Latitude (°N)	Longitude (°E)	Event 1 (m)	Event 2 (m)	Event 3 (m)
16	To Hieu	20.421	106.174	0.4–0.6	0.2–0.4	0.3–0.5
17	Ngo Quyen	20.421	106.176	0.5–0.7	0.3–0.5	0.4–0.6
18	May To 1	20.424	106.177	0.4	0.2	0.3
19	Hang Tien	20.423	106.18	0.3–0.5	0.2–0.4	0.2–0.5
20	Hang Cau	20.432	106.173	0.5–0.7	0.3–0.6	0.4–0.7

2.3. URBAN Model for the Study Area

2.3.1. Catchments

The total catchment area was divided into many sub-catchments. The catchments were set to produce runoff according to a time-area relationship, which is simple and fast owing to its low data requirements. The relationship is based on how large the share of the catchment area is that contributes to runoff after a certain share of rainfall time [47].

2.3.2. Pipe Network

This model was designed for fast computations, enabling the future smart control of the total incoming flow to this basin. Because of this, the pipe network was simplified and represented by the larger main pipes. For the same reason, pumps were excluded. This is likely to have a minor effect on the flow modeling since most of the pipe flow is naturally driven by gravity. The drainage system in the study area was collected and simulated in the MIKE URBAN model (Figure 7).

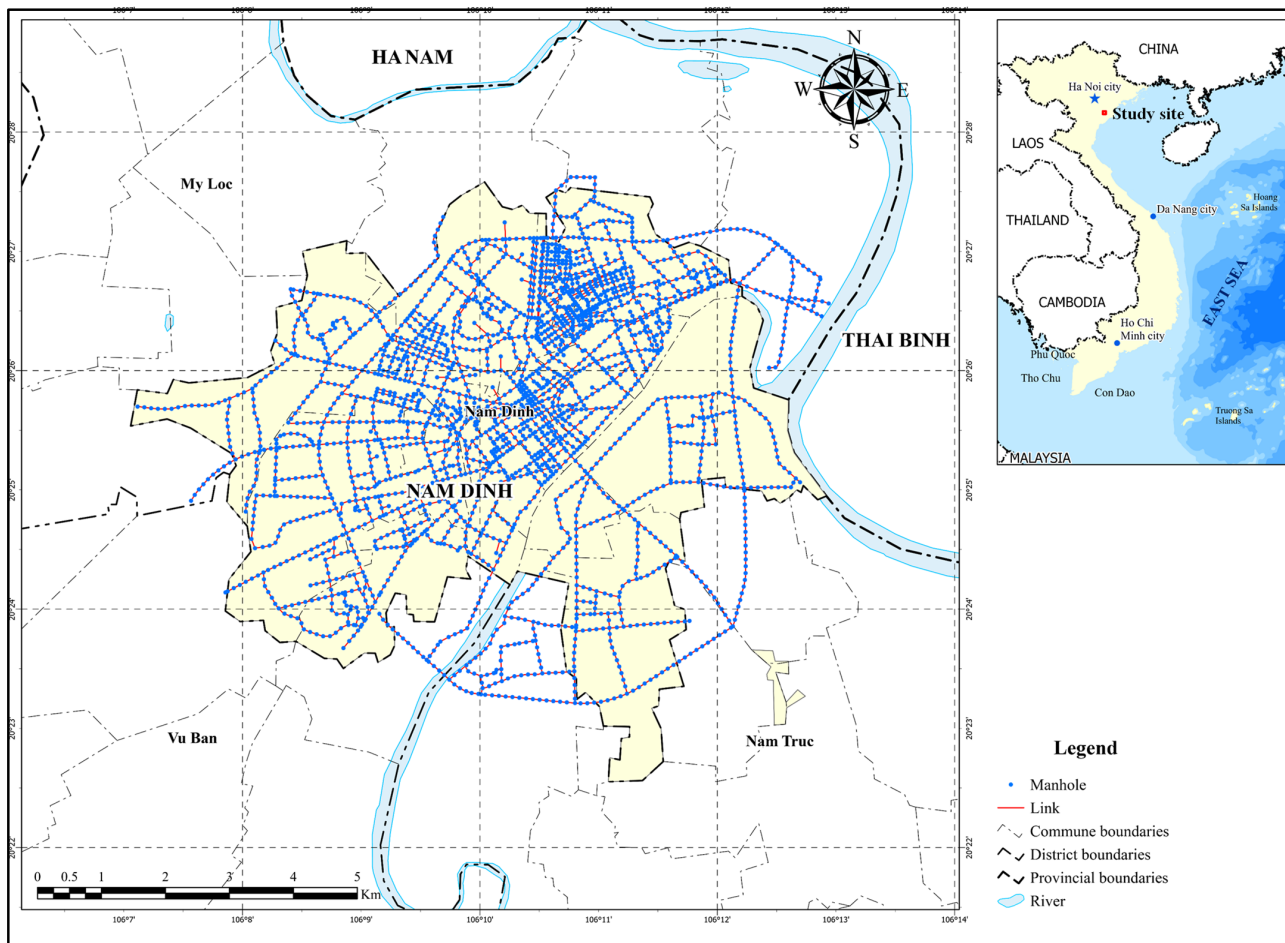


Figure 7. Nam Dinh drainage system in the MIKE URBAN model.

3. Results

3.1. Validation of Precipitation Estimation/Forecasting Precipitation from Radar

Before inputting the QPE and QPF values into the MIKE URBAN model to determine the optimal parameters and simulate flood forecast scenarios for Nam Dinh city, these values are essential to evaluate their performance.

As mentioned in Section 2, the QPE and QPF values were extracted from the locations of four rain gauge stations (namely, Xuan Thuy, Nam Dinh, Lieu De, and Vu Ban) to compare with point-scale rain gauge data during three rainfall events from 2020 to 2022. The first selected event (Event 1) was caused by the influence of the circulation of tropical cyclone (TC) NANGKA accompanied by the impact of a cold air system, and it took place from 10:00 UTC on 13 October 2020 to 09:00 UTC on 15 October 2020. TC NANGKA was an unseasonal TC that landed and greatly affected the south of the Northern Delta region, especially Nam Dinh and Ninh Binh provinces. Damage in Nam Dinh province is valued at approximately 68 VND billion (USD 2.94 million). The second event (Event 2) started around 00:00 UTC on 8 September 2021 and lasted for about 24 h, and it was affected by the Inter Tropical Convergence Zone combined with the easterly wind convergence zone. Event 2 caused heavy rainfall in the Northern Delta region and neighboring provinces. The third one (Event 3) was a heavy rainfall event occurring in the coastal plain and neighboring areas with a common rainfall of 80–150 mm, with maximum rainfall reaching 200 mm in some places, which occurred from 21:00 UTC on 11 August 2022 to 07:00 UTC on 12 August 2022. This event was affected by the circulation of TC MULAN and the Inter Tropical Convergence Zone.

To take an in-depth analysis of the QPE/QPF values, Figures 8–11 show the results of evaluating those values at four rain gauge stations for the three rainfall events mentioned above.

Figure 8a–c show the observed rainfall data (yellow column) along with QPE (black line) and QPF (orange dotted line) at the Xuan Thuy site for three rainfall events, respectively. Overall, the QPE value is relatively close to the observed rainfall than the QPF at the Xuan Thuy site. In Figure 8a (Event 1), QPE and QPF are similar at times of no rain or rain less than 2 mm, which shows that QPE and QPF are not falsely warning at times of no rain in this case. QPE tends to be underestimated at times of heavy rainfall (at 21:00 UTC on 13 October 2020; at 01:00 UTC, 02:00 UTC, 00:00 UTC, and 07:00 UTC on 14 October 2020). QPF tends to be overestimated at times of moderate-intensity rainfall (at 22:00 UTC on 13 October 2020; at 02:00 UTC and 07:00 UTC on 14 October 2020; at 07:00 UTC on 15 October 2020). However, at other times, QPF is also relatively close to the observed rainfall.

In Figure 8b (Event 2), QPE is also overestimated at times of light and moderate rainfall (at 01:00 UTC, 02:00 UTC, 08:00 UTC, and 09:00 UTC on 8 September 2021), but is relatively close to the observation data at times of heavy rainfall (from 19:00 UTC to 23:00 UTC on 8 September 2021). Meanwhile, QPF is overestimated from 01:00 UTC to 03:00 UTC and at 22:00 UTC on 8 September 2021 in this figure. For Event 3, Figure 8c shows that QPE results are very good and close to the observed data, but QPF is overestimated at 23:00 UTC on 11 August 2022 and at 02:00 UTC, 03:00 UTC, and 05:00 UTC on 12 August 2022 (Figure 8c).

Figure 9a–c show the observed rainfall data (yellow column), as well as QPE (black line) and QPF (orange dotted line), at the Nam Dinh site for the three rainfall events, respectively. For Event 3 (Figure 9c), QPE distribution is similar to the observed rainfall distribution, and the peaks of these two distributions occur at the same time at 00:00 UTC on 12 August 2022 and continue to gradually decrease after that point. Thus, this proves that QPE can accurately show a picture of the evolution of rainfall in Nam Dinh city at that time. However, QPE is overestimated compared with the observed data. The QPF in Event 3 also appears to have the same distribution as observed, but the maximum QPF is delayed by one hour compared with the observed maximum rainfall. This can be explained by the fact that, when using the interpolation algorithm from the QPE/QPF radar grid to the site point, it takes the maximum value of the nine grid points surrounding the site location or errors occurring during the process of adjusting the rain intensity estimated from radar with rain gauge data, so the forecasted or estimated value may be distorted, being significantly higher or lower than observed. As described in Section 2.2.1, rainfall

data at Nam Dinh station does not participate in the radar rain gauge adjustment process, which may also be the cause of the high error of QPE at 00:00 UTC on 12 August 2022.

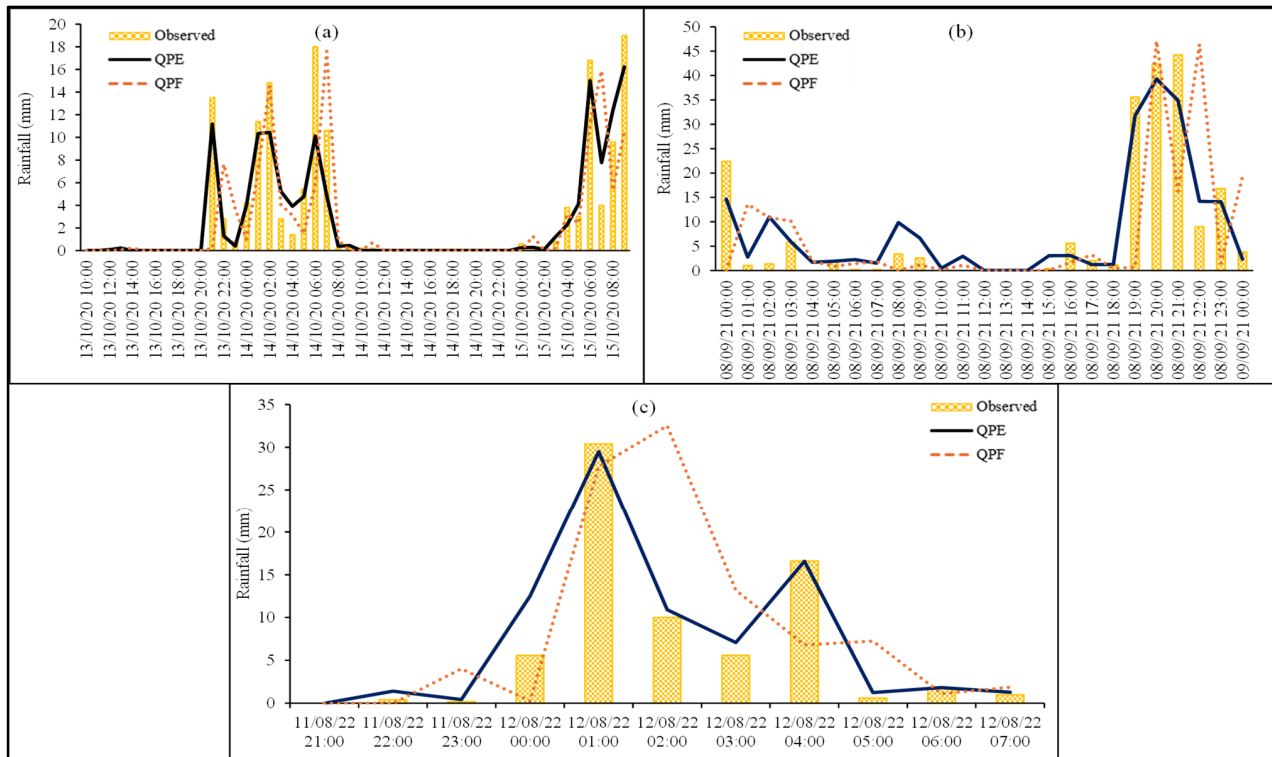


Figure 8. Evaluating QPE and QPF at Xuan Thuy station for the three rainfall events: (a) Event 1, (b) Event 2, (c) Event 3.

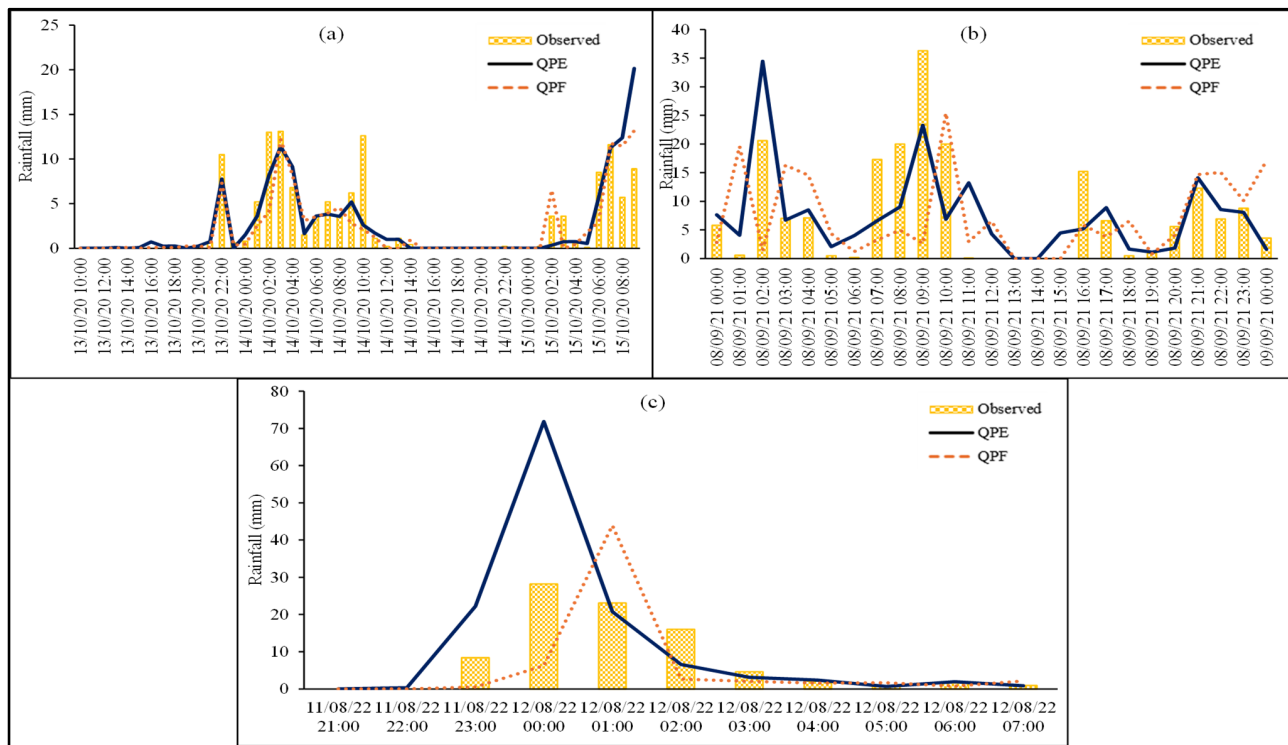


Figure 9. Evaluating QPE and QPF at Nam Dinh station for the three rainfall events: (a) Event 1, (b) Event 2, (c) Event 3.

In Figure 9b (Event 2), QPE is mostly in agreement with the observations, except when it is false at some points (at 1:00 UTC, 2:00 UTC, 5:00 UTC, 11:00 UTC, 12:00 UTC, and 15:00 UTC on 8 September 2021) or underestimated at the time of heaviest rainfall (at 9:00 UTC on 9 September 2021). Also, in this Figure, most QPFs tend to be low compared with the observations, except for the following times: 01:00 UTC, 3:00 UTC–6:00 UTC, 10:00 UTC–12:00 UTC, 18:00 UTC, and 21:00 UTC on 8 September 2021 to 00:00 UTC on 9 September 2021. In Figure 9a, the changes in QPE and QPF are almost identical from the start to the end of Event 2, except at 02:00 UTC on 15 October 2020, when QPF is higher and QPE is smaller compared with the observation.

Figure 10a–c show the observed rainfall data (yellow column) along with QPE (black line) and QPF (orange dotted line) at the Lieu De site for the three rainfall events, respectively.

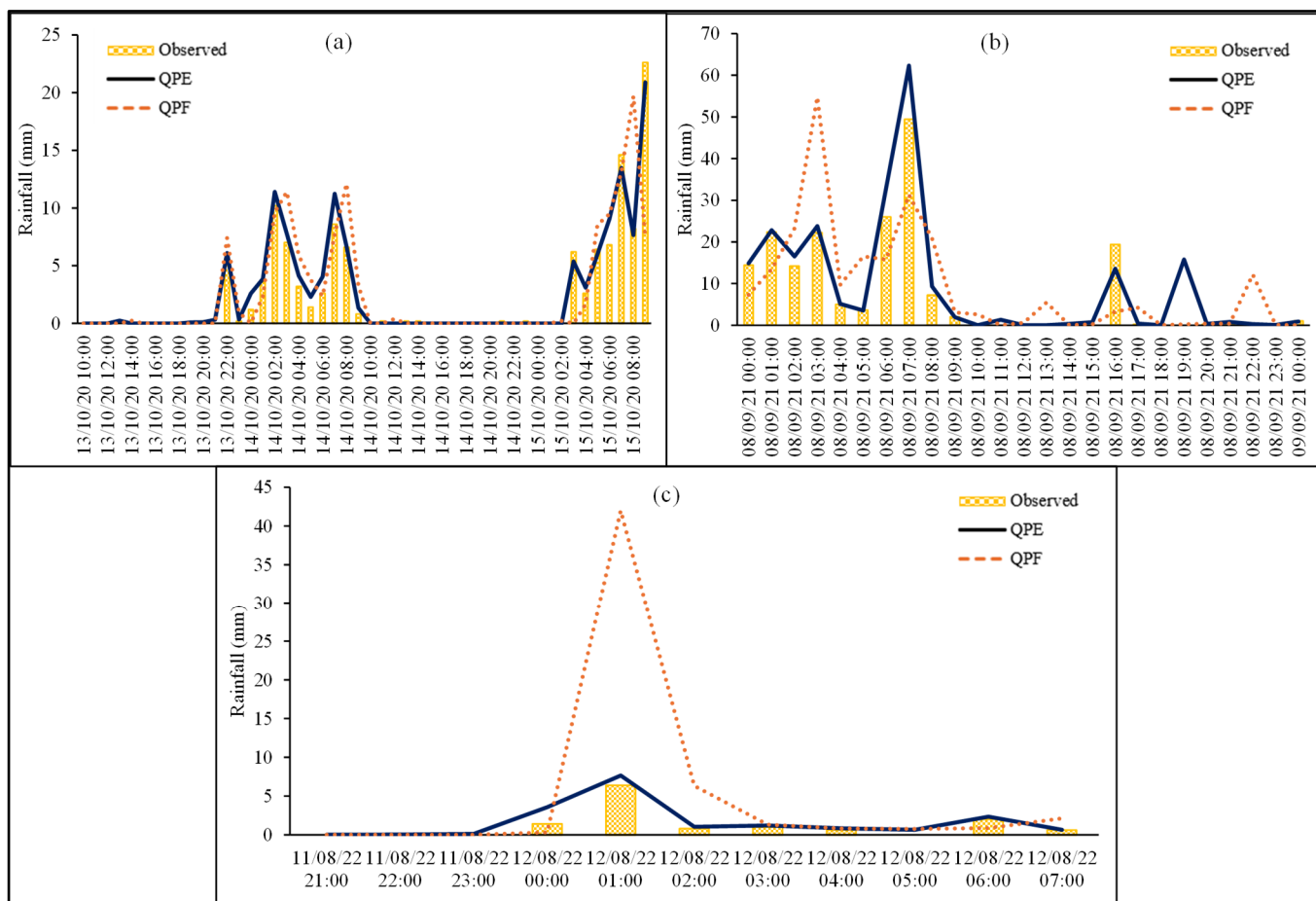


Figure 10. Evaluating QPE and QPF at Lieu De station for the three rainfall events: (a) Event 1, (b) Event 2, (c) Event 3.

The expected QPE and QPF trends in Event 1 are similar, simulating quite closely the observed data at the Lieu De site, except that the time is from 8:00 UTC to 9:00 UTC on 15 October 2020 (Figure 10a). At these times, the expected QPF increase/decrease reports are contrary to reality. In Event 2 and Event 1, QPE also simulates the actual rainfall field quite well at the Lieu De station. In Figure 10b, QPE is relatively close to the observed rainfall occurring at the Lieu De site from the start to the end of Event 2, except at 19:00 UTC on 8 September 2021. Regarding QPF, there are also similarities with QPE, except for 03:00 UTC and 22:00 UTC on the same day. QPE and QPF in Event 3 (Figure 10c) are also closely simulated with the observed values, with the only exception being at 01:00 UTC on 12 August 2022, when QPF is much higher than the observed value. The QPF error may be due to the ROVER_VN optical flow method [31] not capturing the growth or decay process of short-duration rain areas, which is also a limitation of the optical flow method that some

previous studies have mentioned [24], or because the process of estimating the motion of precipitation fields is slower or faster than reality. This can also be seen in Figure 10c (or Figure 11c), in which the predicted QPF values are too high compared to observation at 01:00 UTC on 12 August 2022, while the observed data are too low (Figure 10c) or reach a maximum (Figure 11c) that occurred 1 h before (at 00:00 UTC on 12 August 2022). Therefore, the QPF errors in these figures may be due to the growth/decay process of the rainy area that occurred before the forecast time and the forecast method not being able to catch up. Additionally, both QPE and QPF capture the tendency of this rainfall event quite well.

Similar to the previous figure, Figure 11 shows the evaluation of QPE and QPF against the observed rainfall for the three selected rainfall events at Vu Ban station.

In Event 1, the QPE and QPF at this station are also simulated similarly to those at Lieu De station. It is possible that the characteristics of the observing environment and the topography of these two sites are similar. In particular, QPE and QPF have simulated the developments in rainfall quite well, except from 07:00 UTC to 08:00 UTC on 15 October 2020. The QPE of Event 1 at Vu Ban station is quite close to reality, but QPF may be forecasted to be higher than the actual occurrence at times of moderate rainfall intensity (perhaps because the shifting speed of the forecasted rainfall vector motion field simulation moves slower than actually occurs). Of the three selected rainfall events, Event 1 (13–15 October 2020) is the best case for simulating both the quantitative estimate and the forecasted precipitation fields based on radar. However, the forecasted precipitation field was a false alarm at the time of moderate rainfall intensity (at 01:00 UTC on 12 August 2022) (Figure 11c).

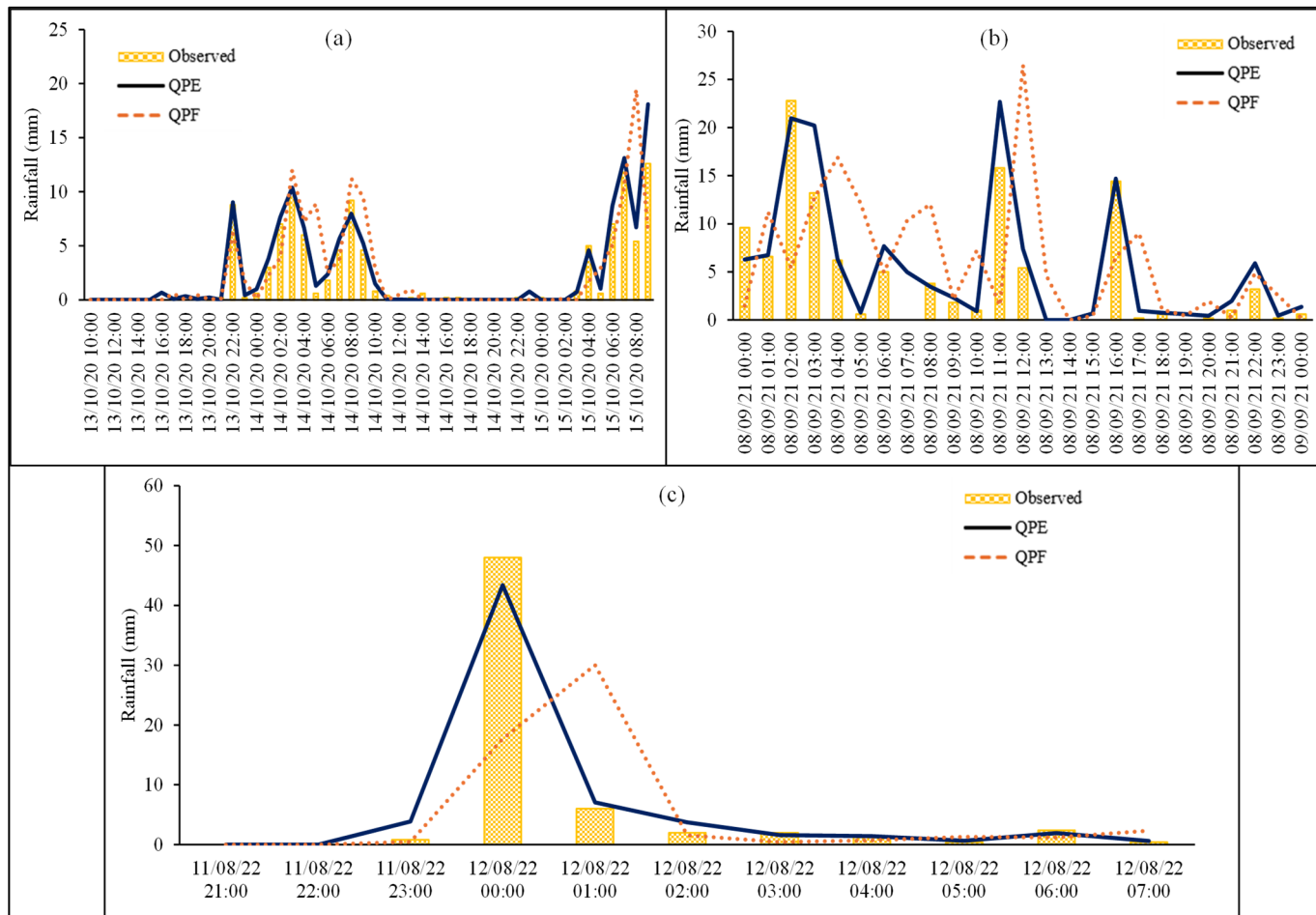


Figure 11. Evaluating QPE and QPF at Vu Ban station for the three rainfall events: **(a)** Event 1, **(b)** Event 2, **(c)** Event 3.

QPE and QPF from the radar are evaluated with observed data at four rain gauge stations, Xuan Thuy, Lieu De, Vu Ban, and Nam Dinh. Among them, data at three rain gauge stations, Xuan Thuy, Lieu De, and Vu Ban, were used for two calibrated steps before calculating QPE. The assessment results of QPE and QPF are higher than the QPE simulation results and QPF at the Nam Dinh station (this station is outside the list of rain gauge stations used to calibrate QPE). The high QPE values may be due to the station point interpolation algorithm or radar rain gauge adjustment steps being used in this study when there is a sudden intensity change in the rain area. QPF tends to have a high bias possibly because the estimate of the motion field of rain particles is shifted more slowly than what actually occurs or due to the ROVER_VN optical flow method not capturing the growth or decay process of short-duration rain areas. In general, the QPE results are relatively good and can be described quite closely to the reality occurring at these four rain gauge stations. Therefore, using QPE and QPF data from radar in hydrological models is positive and can be applied in Vietnam.

3.2. Calibration and Validation Results of the MIKE URBAN Model

After QPE and QPF were validated, this study selected two heavy rainfalls (Event 1 and Event 2) to simulate inundation for Nam Dinh city. The inundation survey locations were used to calibrate and validate the MIKE URBAN model for the study area. The calibration and validation results are shown in Tables 2 and 3 and Figure 12. The calibration and validation results show that an error assessment between an observed and simulated water depth at 20 survey locations was arranged from 0–0.05 m to 0–0.08 m, respectively (Tables 2 and 3).

Table 2. Error assessment of calibration (Event 1).

No.	ID	Location	Lat (°N)	Long (°E)	Observed (m)	Simulated (m)	ΔH (m)
1	ND1	Vi Hoang	20.434	106.179	0.4	0.47	0.07
2	ND2	Nguyen Du	20.433	106.182	0.5	0.55	0.05
3	ND3	Tran Hung Dao	20.432	106.173	0.75	0.81	0.06
4	ND4	Ly Thuong Kiet	20.431	106.173	0.5	0.47	-0.03
5	ND5	Luong Van Can	20.444	106.186	0.3	0.35	0.05
6	ND6	Luong The Vinh	20.427	106.165	0.2	0.18	-0.02
7	ND7	Doan Tran Nghiep	20.426	106.166	0.35	0.35	0
8	ND8	Tran Dang Ninh	20.423	106.165	0.5	0.49	-0.01
9	ND9	Tran Binh San	20.412	106.167	0.4	0.4	0
10	ND10	Han Thuyen	20.437	106.183	0.65	0.69	0.04
11	ND11	Le Hong Son	20.427	106.168	0.35	0.32	-0.03
12	ND12	Le Hong Phong	20.43	106.182	0.4	0.34	-0.06
13	ND13	Tran Quang Khai	20.409	106.168	0.35	0.3	-0.05
14	ND14	Cau Do Quan	20.424	106.178	0.5	0.47	-0.03
15	ND15	Hang Thao	20.423	106.177	0.65	0.65	0
16	ND16	To Hieu	20.421	106.174	0.5	0.5	0
17	ND17	Ngo Quyen	20.421	106.176	0.6	0.55	-0.05
18	ND18	May To	20.424	106.177	0.85	0.88	0.03
19	ND19	Hang Tien	20.434	106.176	0.4	0.36	-0.04
20	ND20	Hang Cau	20.423	106.18	0.6	0.52	-0.08

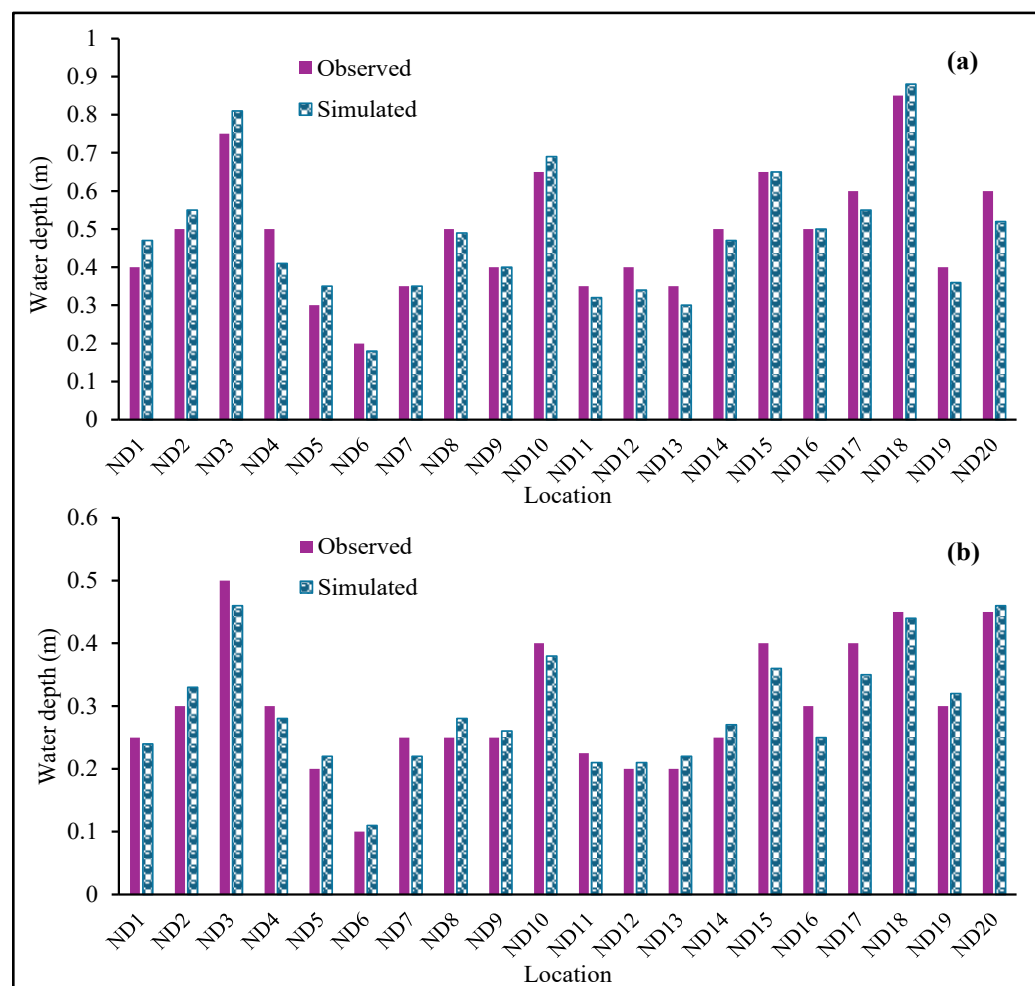
Table 3. Error assessment of validation (Event 2).

No.	ID	Location	Lat (°N)	Long (°E)	Observed (m)	Simulated (m)	ΔH (m)
1	ND1	Vi Hoang	20.434	106.179	0.25	0.24	-0.01
2	ND2	Nguyen Du	20.433	106.182	0.3	0.33	0.03
3	ND3	Tran Hung Dao	20.432	106.173	0.5	0.46	-0.04

Table 3. Cont.

No.	ID	Location	Lat (°N)	Long (°E)	Observed (m)	Simulated (m)	ΔH (m)
4	ND4	Ly Thuong Kiet	20.431	106.173	0.3	0.28	-0.02
5	ND5	Luong Van Can	20.444	106.186	0.2	0.22	0.02
6	ND6	Luong The Vinh	20.427	106.165	0.1	0.11	0.01
7	ND7	Doan Tran Nghiep	20.426	106.166	0.25	0.22	-0.03
8	ND8	Tran Dang Ninh	20.423	106.165	0.25	0.28	0.03
9	ND9	Tran Binh San	20.412	106.167	0.25	0.26	0.01
10	ND10	Han Thuyen	20.437	106.183	0.4	0.38	-0.02
11	ND11	Le Hong Son	20.427	106.168	0.225	0.21	-0.015
12	ND12	Le Hong Phong	20.43	106.182	0.2	0.21	0.01
13	ND13	Tran Quang Khai	20.409	106.168	0.2	0.22	0.02
14	ND14	Cau Do Quan	20.424	106.178	0.25	0.27	0.02
15	ND15	Hang Thao	20.423	106.177	0.4	0.36	-0.04
16	ND16	To Hieu	20.421	106.174	0.3	0.25	-0.05
17	ND17	Ngo Quyen	20.421	106.176	0.4	0.35	-0.05
18	ND18	May To	20.424	106.177	0.45	0.44	-0.01
19	ND19	Hang Tien	20.434	106.176	0.3	0.32	0.02
20	ND20	Hang Cau	20.423	106.18	0.45	0.46	0.01

The results of assessing the error between the inundation depth at the survey location and the simulated inundation from the MIKE URBAN model are shown in Figure 12a,b.

**Figure 12.** Results of water depth: (a) calibration, (b) validation.

The results of the calibration and validation model provide a relatively consistent assessment with an average flooding depth error of 0.05–0.06 m. Therefore, the parameter set of the MIKE URBAN model will be continued to calculate for simulation scenarios with rainfall gauge data and radar data (Table 4).

Table 4. The parameters set of the MIKE URBAN model.

No.	Parameters	Value
1	Imperviousness (%) +River, lake +Building, road +Other	100 80 30
2	Discharge coefficient	0.98
3	Time of concentration (min)	5–10
4	Initial loss (m)	0.0006
5	Reduction factor	0.75
6	Manning ($m^{1/3}/s$)	85

3.3. Results of the Inundation Simulation

After the calibration and validation of the MIKE URBAN model parameters for the study area, this study used forecast rainfall data from radar (QPF) and forecast rainfall data at Nam Dinh station to simulate an inundation forecast for Nam Dinh city. Below are the simulation results for Event 3. Two simulation scenarios were set up as follows:

- Scenario 1: Simulate an inundation forecast for Nam Dinh city with the input being forecast rainfall at Nam Dinh hydrological station (Scenario 1).
- Scenario 2: Simulate an inundation forecast for Nam Dinh city with the input being QPF data (Scenario 2).

Figure 13a–c show the results of the water-depth-simulated scenarios and the surveyed water depth at 20 survey locations (Figure 13a). The relative error between the two scenarios is shown in Figure 13b, and the difference in water depth between the two scenarios with the survey value is shown in Figure 13c.

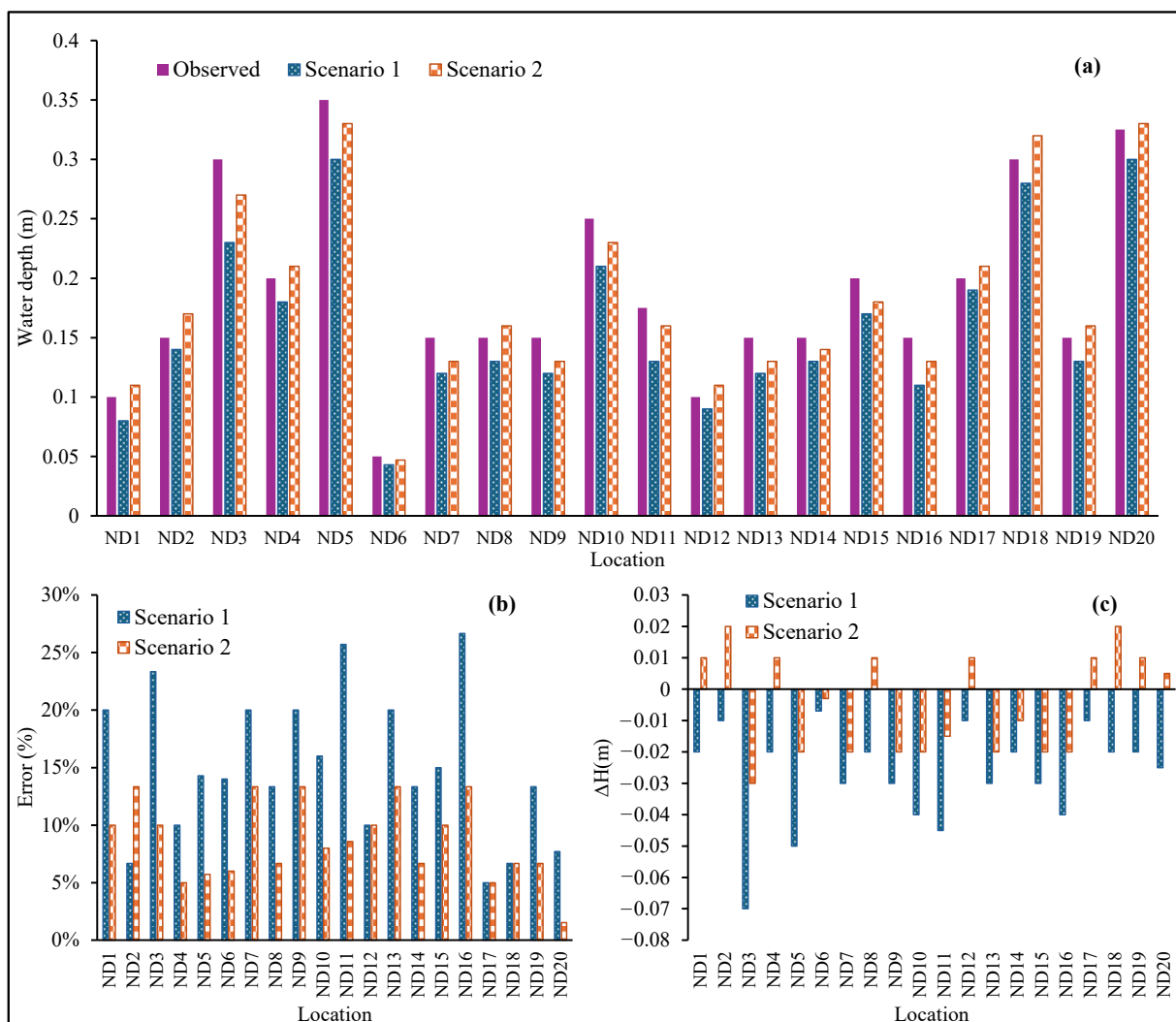
The results in Table 5 and Figure 13 show that Scenario 2 with rainfall forecast data from radar provides better simulation results. The average relative error in Scenario 2 is 9%, while the average relative error in Scenario 1 is 15%. The average flood depth difference is 0.03 m in Scenario 1 and Scenario 2 is 0.005 m in Scenario 2. This result initially shows that using a grid model as input data for the MIKE URBAN model increases the simulation accuracy of the model. The error between the observed water depth and the simulated results with QPF input has decreased for the simulation when using input forecasted rainfall at Nam Dinh station.

Table 5. Comparison of the simulation results from forecasted rain in Scenario 1 and Scenario 2.

No	ID	Location	Lat (°N)	Long (°E)	Observed (m)	Scenario 1			Scenario 2		
						Simulated	ΔH (m)	Error (%)	Simulated	ΔH (m)	Error (%)
1	ND1	Vi Hoang	20.434	106.179	0.1	0.08	−0.02	20%	0.11	0.01	10%
2	ND2	Nguyen Du	20.433	106.182	0.15	0.14	−0.01	7%	0.17	0.02	13%
3	ND3	Tran Hung Dao	20.432	106.173	0.3	0.23	−0.07	23%	0.27	−0.03	10%
4	ND4	Ly Thuong Kiet	20.431	106.173	0.2	0.18	−0.02	10%	0.21	0.01	5%
5	ND5	Luong Van Can	20.444	106.186	0.35	0.3	−0.05	14%	0.33	−0.02	6%
6	ND6	Luong The Vinh	20.427	106.165	0.05	0.043	−0.007	14%	0.047	−0.003	6%
7	ND7	Doan Tran Nghiep	20.426	106.166	0.15	0.12	−0.03	20%	0.13	−0.02	13%
8	ND8	Tran Dang Ninh	20.423	106.165	0.15	0.13	−0.02	13%	0.16	0.01	7%
9	ND9	Tran Binh San	20.412	106.167	0.15	0.12	−0.03	20%	0.13	−0.02	13%
10	ND10	Han Thuyen	20.437	106.183	0.25	0.21	−0.04	16%	0.23	−0.02	8%
11	ND11	Le Hong Son	20.427	106.168	0.175	0.13	−0.045	26%	0.16	−0.015	9%
12	ND12	Le Hong Phong	20.43	106.182	0.1	0.09	−0.01	10%	0.11	0.01	10%
13	ND13	Tran Quang Khai	20.409	106.168	0.15	0.12	−0.03	20%	0.13	−0.02	13%
14	ND14	Cau Do Quan	20.424	106.178	0.15	0.13	−0.02	13%	0.14	−0.01	7%
15	ND15	Hang Thao	20.423	106.177	0.2	0.17	−0.03	15%	0.18	−0.02	10%

Table 5. Cont.

No	ID	Location	Lat (°N)	Long (°E)	Observed (m)	Scenario 1			Scenario 2		
						Simulated	ΔH (m)	Error (%)	Simulated	ΔH (m)	Error (%)
16	ND16	To Hieu	20.421	106.174	0.15	0.11	-0.04	27%	0.13	-0.02	13%
17	ND17	Ngo Quyen	20.421	106.176	0.2	0.19	-0.01	5%	0.21	0.01	5%
18	ND18	May To	20.424	106.177	0.3	0.28	-0.02	7%	0.32	0.02	7%
19	ND19	Hang Tien	20.434	106.176	0.15	0.13	-0.02	13%	0.16	0.01	7%
20	ND20	Hang Cau	20.423	106.18	0.325	0.3	-0.025	8%	0.33	0.005	2%

**Figure 13.** Simulated and observed results error from the two scenarios: (a) water depth, (b) error (%), (c) the difference in water depth between the two scenarios with the survey value (ΔH).

The results from the MIKE URBAN model in Scenario 1 are low because the rainfall data used for the simulation were taken from a station in the city center; therefore, in areas far away from that rain gauge station, the results will be lower. The simulations tended to gradually decrease in accuracy, especially in the southern area of Nam Dinh city, where there are many rice fields with lower terrain, so Scenario 1 did not simulate it correctly (Figure 14a).

Scenario 2 simulated gridded radar rain data covering the entirety of Nam Dinh city. The results show that the water depth is more accurate than in Scenario 1. The model also simulated more accurately in space because it can simulate the southern area of the city where there are many low fields more precisely (Figure 14b).

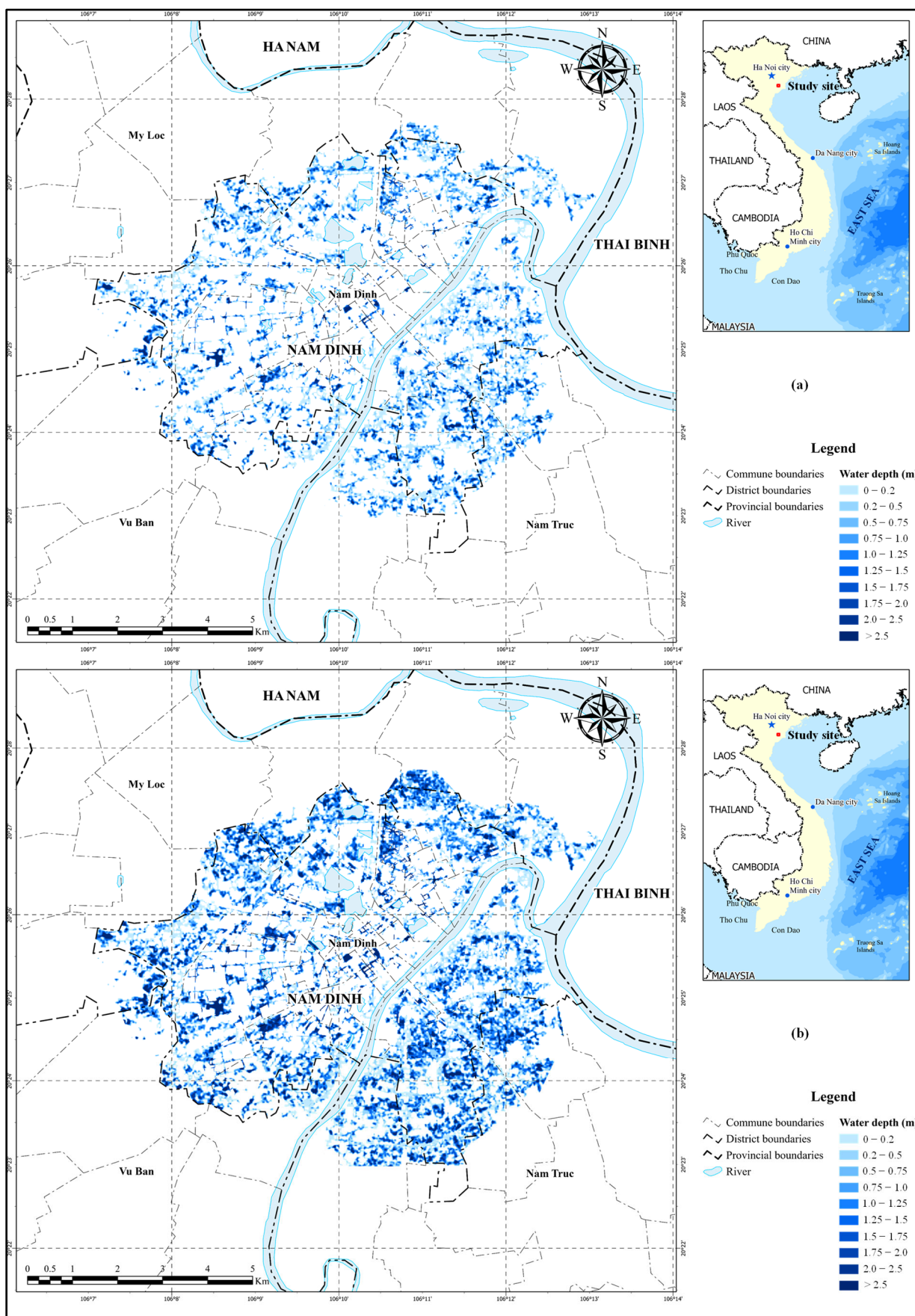


Figure 14. Inundation map of Nam Dinh city: (a) Scenario 1, (b) Scenario 2.

4. Discussion

In this section, the points from the previously concluded analysis of the simulation results are discussed, along with the usage and possibilities of the radar and its data. As mentioned above, using QPE and QPF data as inputs for a hydrological model to simulate urban flooding in Nam Dinh province provided good results and was found to be suitable for the actual occurrence. The QPF results are good when QPE is good [52]. The QPE and QPF results extracted from the grid for each station also contribute significantly to simulating flooding in hydrological models. In the case that used the method of extracting from the grid to the station by taking the largest value of the nine grid points around the station location, most of the extraction results were much better than those obtained from extracting the exact location of the station point. However, there are also limitations in the cases where the rainfall at the station at that time reaches its peak because in these cases, the rainfall tends to be estimated as higher than the actual observation. This leads to forecast results that tend to be higher than the actual occurrence [31]. Most case studies show that because the QPF method uses the ROVER_VN optical flow technique, in which the forecast uses the backward semi-Lagrangian extrapolation method [31], the forecasted field does not fully describe the development and weakening process of rainy areas, leading to a tendency for the forecasted precipitation field to deviate greatly from reality during extreme rainfall and lead-time long-term forecasting [53–58].

According to the plans for the area, Nam Dinh province is to become a province of rapid, comprehensive, and sustainable development; it is one of the most developed provinces in the country, and it is one of the most important development centers in the Southern Red River Delta region. Nam Dinh city is a grade I urban area in Nam Dinh province. When heavy rain occurs continuously in Nam Dinh, a series of streets and residential areas in the city become deeply flooded with water, causing traffic chaos. Many houses become flooded with water, many businesses have to close, and many students cannot go to school. Many officials, public employees, workers, and laborers struggled or could not get to work. This is also a common situation in many urban areas in Vietnam whenever heavy rain occurs. This study uses the rainfall from radar as input for the MIKE URBAN model to simulate and forecast inundation and flooding. The inundation calculation results for Nam Dinh city for two simulation scenarios show the effectiveness of including the application of rain radar in the forecasting and warning of urban floods. This is also the first study to apply rain radar to evaluate the effectiveness of flood forecasting and warning for Nam Dinh city. These study results using the rain radar as an input for the MIKE URBAN model will be used as the basis for establishing an operational forecasting system for the Northern Delta and Midland Regional Hydro-Meteorological Center, Viet Nam Meteorological and Hydrological Administration, to be tested in 2024 and transferred and applied in 2025. When put into operation, the system will provide great support for forecasters for their operations and early warning messages for people to improve the prevention and mitigation of damage caused by flooding [59–63].

5. Conclusions

This study evaluated the usage of rain radar data as inputs for the MIKE URBAN model. One of the most prominent strengths is its spatial coverage, which simulated inundation in the city's southern areas when rain gauge data were used. This information can be of great value in cases of higher-intensity local rainfall. The main findings of the results are summarized as follows:

- QPE and QPF products with high temporal and spatial resolution are reliable products that could respond well to daily operations. They were inputs used to replace traditional precipitation data when applied in hydrological and hydraulic models to simulate urban inundation in the event of heavy rain in Nam Dinh city.
- This study successfully applied QPE data to the MIKE URBAN model to find the optimal set of parameters for forecasting and warning of inundation in Nam Dinh city in specific study cases.

- This study applied a set of selected parameters to simulate the water level of inundation in Nam Dinh city in two scenarios. The error of the average inundation depth when applying QPF data to the MIKE URBAN model for Nam Dinh city area (Scenario 2) is quite small compared to using forecast data from a single hydrological station (Scenario 1).

Research and development of urban inundation forecasting scenarios considering the impact of climate change will be another problem that will be further studied in urban planning. However, it is possible to update additional drainage works in the MIKE URBAN modeling system based on development planning and calculate future forecasting scenarios with climate change inputs.

In the future, this study's results will contribute to improving the quality of forecasting and warnings of inundation and floods in Nam Dinh city, especially at the Northern Delta and Midland Regional Hydro-Meteorological Center, Viet Nam Meteorological and Hydrological Administration. It is a premise for future research applying QPE and QPF data from radar to simulate flooding in other urban areas in Vietnam. Therefore, this result will be integrated into the early warning system for the Nam Dinh Provincial Hydro-Meteorological Station. As soon as forecast precipitation data are available, a flood risk warning map will be issued. Based on this result, the forecaster will provide warning bulletins to relevant agencies and managers to come up with appropriate response methods, such as directing traffic to avoid potentially dangerous road sections with a high flooding capacity, checking the condition of drainage manhole covers, etc.

Author Contributions: Conceptualization, D.Q.T., N.V.T., B.T.K.H., H.A.N.-T., V.V.H., L.T.H. and H.T.T.P.; methodology, D.Q.T., N.V.T., B.T.K.H., H.A.N.-T., V.V.H., D.T.D. and L.T.H.; software, D.Q.T. and B.T.K.H.; calibration and validation, D.Q.T. and B.T.K.H.; formal analysis, N.V.T., B.T.K.H., H.A.N.-T., V.V.H., D.T.D. and L.T.H.; investigation, D.Q.T., N.V.T., B.T.K.H., H.A.N.-T., V.V.H., L.T.H., D.T.D. and H.T.T.P.; data curation, N.V.T., B.T.K.H., H.A.N.-T., V.V.H., D.T.D. and L.T.H.; writing—original draft preparation, D.Q.T., N.V.T., B.T.K.H., H.A.N.-T., V.V.H., L.T.H. and H.T.T.P.; writing—review and editing, D.Q.T., B.T.K.H. and H.T.T.P.; visualization, D.Q.T., N.V.T., B.T.K.H., H.A.N.-T., V.V.H., L.T.H. and H.T.T.P. All authors have read and agreed to the published version of the manuscript.

Funding: This research was funded by the National Research Project under the Ministry of Science and Technology of Vietnam titled “Research on the application of optical flow technique to the quantitative estimation and quantitative forecast of precipitation in Vietnam based on Himawari satellite and weather radar data” with grant code ĐTDL.CN-58/21 and the Ministry project “Research on building a flood warning system due to heavy rains based on a combined forecasting approach for some urban areas in the Northern Delta region”, code TNMT.2023.06.04.

Institutional Review Board Statement: Not applicable.

Informed Consent Statement: Not applicable.

Data Availability Statement: All data are in the manuscript.

Conflicts of Interest: The authors declare no conflicts of interest.

References

1. Gilewski, P.; Nawalany, M. Inter-comparison of rain-gauge, radar, and satellite (IMERG GPM) precipitation estimates performance for rainfall-runoff modeling in a mountainous catchment in Poland. *Water* **2018**, *10*, 1665. [[CrossRef](#)]
2. McKee, J.L.; Binns, A.D. A review of gauge-radar merging methods for quantitative precipitation estimation in hydrology. *Can. Water Resour. J.* **2016**, *41*, 186–203. [[CrossRef](#)]
3. Gabriele, S.; Chiaravalloti, F.; Procopio, A. Radar-rain-gauge rainfall estimation for hydrological applications in small catchments. *Adv. Geosci.* **2017**, *44*, 61–66. [[CrossRef](#)]
4. Hasan, M.M.; Sharma, A.; Johnson, F.; Mariethoz, G.; Seed, A. Correcting bias in radar Z–R relationships due to uncertainty in point rain gauge networks. *J. Hydrol.* **2014**, *519*, 1668–1676. [[CrossRef](#)]
5. Dai, Q.; Yang, Q.; Zhang, J.; Zhang, S. Impact of gauge representative error on a radar rainfall uncertainty model. *J. Appl. Meteorol. Climatol.* **2018**, *57*, 2769–2787. [[CrossRef](#)]

6. Tang, G.; Behrangi, A.; Long, D.; Li, C.; Hong, Y. Accounting for spatiotemporal errors of gauges: A critical step to evaluate gridded precipitation products. *J. Hydrol.* **2018**, *559*, 294–306. [[CrossRef](#)]
7. Sokol, Z.; Szturc, J.; Orellana-Alvear, J.; Popová, J.; Jurczyk, A.; Céller, R. The role of weather radar in rainfall estimation and its application in meteorological and hydrological modelling: A review. *Remote Sens.* **2021**, *13*, 351. [[CrossRef](#)]
8. Moreno, H.A.; Vivoni, E.R.; Gochis, D.J. Utility of quantitative precipitation estimates for high resolution hydrologic forecasts in mountain watersheds of the Colorado front range. *J. Hydrol.* **2012**, *438–439*, 66–83. [[CrossRef](#)]
9. McMillan, H.; Jackson, B.; Clark, M.; Kavetski, D.; Woods, R. Rainfall uncertainty in hydrological modelling: An evaluation of multiplicative error models. *J. Hydrol.* **2011**, *400*, 83–94. [[CrossRef](#)]
10. Mapiam, P.P.; Sriwongsitanon, N.; Chumchean, S.; Sharma, A. Effects of rain gauge temporal resolution on the specification of a Z–R relationship. *J. Atmos. Ocean. Technol.* **2009**, *26*, 1302–1314. [[CrossRef](#)]
11. Wang, L.P.; Ochoa-Rodriguez, S.; Assel, J.V.; Pina, R.D.; Pessemier, M.; Kroll, S.; Willems, P.; Onof, C. Enhancement of radar rainfall estimates for urban hydrology through optical flow temporal interpolation and Bayesian gauge-based adjustment. *J. Hydrol.* **2015**, *531*, 408–426. [[CrossRef](#)]
12. Goudenhoofdt, E.; Delobbe, L. Evaluation of radar-gauge merging methods for quantitative precipitation estimates. *Hydrol. Earth Syst. Sci.* **2009**, *13*, 195–203. [[CrossRef](#)]
13. Falck, A.S.; Maggioni, V.; Tomasella, J.; Diniz, F.L.R.; Mei, Y.; Beneti, C.A.; Herdies, D.L.; Neundorf, R.; Caram, R.O.; Rodriguez, D.A. Improving the use of ground-based radar rainfall data for monitoring and predicting floods in the Iguaçu river basin. *J. Hydrol.* **2018**, *567*, 626–636. [[CrossRef](#)]
14. Ochoa-Rodriguez, S.; Wang, L.P.; Willems, P.; Onof, C. A Review of radar-rain gauge data merging methods and their potential for urban hydrological applications. *Water Resour. Res.* **2019**, *55*, 6356–6391. [[CrossRef](#)]
15. Kimpara, C.; Tonouchi, M.; Hoa, B.T.K.; Hung, N.V.; Cuong, N.M.; Akaeda, K. Evaluation of the radar-based quantitative precipitation estimation composite in Viet Nam. *J. Hydrometeorol.* **2023**, *15*, 28–39. [[CrossRef](#)]
16. Roversi, G.; Pancaldi, M.; Cossich, W.; Corradini, D.; Nguyen, T.T.N.; Nguyen, T.V.; Porcu', F. The extreme rainfall events of the 2020 typhoon season in Vietnam as seen by seven different precipitation products. *Remote Sens.* **2024**, *16*, 805. [[CrossRef](#)]
17. Kimpara, C.; Tonouchi, M.; Hoa, B.T.K.; Hung, N.V.; Cuong, N.M.; Akaeda, K. Quantitative precipitation estimation by combining rain gauge and meteorological radar network in Viet Nam. *VN J. Hydrometeorol.* **2020**, *5*, 36–50. [[CrossRef](#)]
18. Makihara, Y. A method for improving radar estimates of precipitation by comparing data from radars and rain gauges. *J. Meteor. Soc. Jpn.* **1996**, *74*, 459–480. [[CrossRef](#)]
19. Rossa, A.; Liechti, K.; Zappa, M.; Bruen, M.; Germann, U.; Haase, G.; Keil, C.; Krahe, P. The COST 731 action: A review on uncertainty propagation in advanced hydro-meteorological forecast systems. *Atmos. Res.* **2011**, *100*, 150–167. [[CrossRef](#)]
20. Van Steenbergen, N.; Willems, P. Rainfall uncertainty in flood forecasting: Belgian case study of Rivierbeek. *J. Hydrol. Eng.* **2014**, *19*, 05014013-1–05014013-6. [[CrossRef](#)]
21. Cloke, H.L.; Pappenberger, F. Ensemble flood forecasting: A review. *J. Hydrol.* **2009**, *375*, 613–626. [[CrossRef](#)]
22. Zappa, M.; Jaun, S.; Germann, U.; Walser, A.; Fundel, F. Superposition of three sources of uncertainties in operational flood forecasting chains. *Atmos. Res.* **2011**, *100*, 246–262. [[CrossRef](#)]
23. Fabry, F.; Seed, A. Quantifying and predicting the accuracy of radar-based quantitative precipitation forecasts. *Adv. Water Resour.* **2009**, *32*, 1043–1049. [[CrossRef](#)]
24. Woo, W.C.; Wong, W.K. Operational application of optical flow techniques to radar-based rainfall nowcasting. *Atmosphere* **2017**, *8*, 48. [[CrossRef](#)]
25. Bowler, N.E.H.; Pierce, C.E.; Seed, A. Development of a precipitation nowcasting algorithm based upon optical flow techniques. *J. Hydrol.* **2004**, *288*, 74–91. [[CrossRef](#)]
26. Bowler, N.E.; Pierce, C.E.; Seed, A.W. STEPS: A probabilistic precipitation forecasting scheme which merges an extrapolation nowcast with downscaled NWP. *Q. J. R. Meteorolog. Shock.* **2006**, *132*, 2127–2155. [[CrossRef](#)]
27. Bellon, A.; Zawadzki, I.; Kilambi, A.; Lee, H.C.; Hee Lee, Y.; Gyuwon Lee, G. McGill algorithm for precipitation nowcasting by Lagrangian extrapolation (MAPLE) applied to the South Korean radar network. Part I: Sensitivity studies of the variational echo tracking (VET) technique. *Asia-Pac. J. Atmos. Sci.* **2010**, *46*, 369–381. [[CrossRef](#)]
28. Lee, H.C.; Lee, Y.H.; Ha, J.C.; Chang, D.E.; Bellon, A.; Zawadzki, I.; Lee, G. McGill algorithm for precipitation nowcasting by Lagrangian extrapolation (MAPLE) applied to the South Korean radar network. Part II: Real-time verification for the summer season. *Asia-Pac. J. Atmos. Sci.* **2010**, *46*, 383–391. [[CrossRef](#)]
29. Li, P.W.; Lai, S.T. Applications of radar-based nowcasting techniques for mesoscale weather forecasting in Hong Kong. *Meteorol. Appl.* **2004**, *11*, 253–264. [[CrossRef](#)]
30. Novák, P.; Březková, L.; Frolík, P. Quantitative precipitation forecast using radar echo extrapolation. *Atmos. Res.* **2009**, *93*, 328–334. [[CrossRef](#)]
31. Thu, N.V.; Tri, D.Q.; Hoa, B.T.K.; Nguyen-Thi, H.A.; Hung, N.V.; Tuyet, Q.T.T.; Nhat, N.V.; Pham, H.T.T. Application of optical flow technique to short-term rainfall forecast for some synoptic patterns in Vietnam. *Theor. Appl. Climatol.* **2024**, preprint. [[CrossRef](#)]
32. Goenner, A.R.; Franz, K.J.; Gallus, W.A., Jr.; Roberts, B. Evaluation of an application of probabilistic quantitative precipitation forecasts for flood forecasting. *Water* **2020**, *12*, 2860. [[CrossRef](#)]
33. Mark, O.; Jørgensen, C.; Hammond, M.; Khan, D.; Tjener, R.; Erichsen, A.; Helwigh, B. A new methodology for modelling of health risk from urban flooding exemplified by Cholera—Case Dhaka, Bangladesh. *J. Flood Risk Manag.* **2018**, *11*, S28–S42. [[CrossRef](#)]

34. Chen, A.S.; Hammond, M.J.; Djordjević, S.; Butler, D.; Khan, D.M.; Veerbeek, W. *From Hazard to Impact: Flood Damage Assessment tools for Mega Cities*; Springer Nature: Berlin/Heidelberg, Germany, 2016; p. 82. ISBN 1106901622.
35. Luan, Q.; Zhang, K.; Liu, J.; Wang, D.; Ma, J. The application of MIKE URBAN model in drainage and waterlogging in Lincheng county, China. *Proc. IAHS* **2018**, *379*, 381–386. [CrossRef]
36. Yin, L.; Shuanghu, Z.; Huidong, S.; Dan, W.; Qihao, G. Modelling and application of urban drainage based on MIKE URBAN mode. *IOP Conf. Ser. Earth Environ. Sci.* **2020**, *474*, 062003. [CrossRef]
37. Olsson, L. Flow Simulation in MIKE URBAN Based on High-Resolution X-Band Radar Data. A Case Study in Lund. Master’s Thesis, Lund University, Lund, Sweden, 2019; p. 72.
38. Dung, L.D. Assessment of climate change impact on floods risk in the inner city of Hanoi. *J. Hydro-Meteorol.* **2016**, *670*, 7–12. (In Vietnamese)
39. Binh, N.Q.; Hung, N.T.; Chinh, L.Q. Application of MIKE URBAN model to calculate water supply network of TamKy city according to orientation planning by 2030. *J. Sci. Technol. Univ. Danang* **2016**, *7*, 6–10.
40. Doan, P.T.K.; Le, X.C.; Le, V.T.; Némery, J. Evaluating the impacts of an improved sewer system on city flood inundations using MIKE Urban Model. *VN J. Earth Sci.* **2023**, *45*, 438–455. [CrossRef]
41. Hung, N.Q.; Lien, N.T. Application of urban hydrology model and green design for the drainage system of Ha Tinh City. *VNU J. Sci. Earth Environ. Sci.* **2021**, *37*, 50–62.
42. Dai, N.V.; Nam, N.A.; Thinh, D.Q.; Hiep, N.V.; Tuan, P.V. Establishing an urban inundation forecast system for Hanoi area using high resolution grid rainfall data. *J. Clim. Change Sci.* **2019**, *12*, 32–41.
43. Available online: <https://www.vietnam.vn/en/thanh-pho-nam-dinh-chu-dong-nang-cao-nang-luc-thoat-nuoc-do-thi/> (accessed on 3 June 2023).
44. Available online: <https://sotnmt.namdinh.gov.vn/vi-vn/tin-tuc/ban-tin-du-bao-thoi-tiet/220> (accessed on 3 June 2023).
45. Dai, N.V.; Tuyen, N.K.; Thinh, D.Q.; Long, P.B. Impacts of climate change on inundation in Nam Dinh city. *J. Clim. Change Sci.* **2018**, *5*, 51–58. (In Vietnamese)
46. Trung, N.X.; Lee, S.I. Flood and land losses in northern Vietnam due to climate change and sea level rise. *Int. J. Innov. Res. Sci. Eng. Technol.* **2013**, *2*, 7061–7067.
47. MIKE URBAN. Collection System, 2014. Available online: <https://manuals.mikepoweredbydhi.help/2017/Cities/CollectionSystem.pdf> (accessed on 31 December 2017).
48. Available online: https://www.geography.at/study/analysis/cadus_poetsch_seminar-paper.pdf (accessed on 8 March 2012).
49. WMO. Guide to Meteorological Instruments and Methods of Observation. 2014. Available online: https://library.wmo.int/doc_num.php?explnum_id=4147 (accessed on 11 March 2019).
50. Shroder, J. Chapter 11—Issues of Hydrologic Data Collection by Remote Sensing in Afghanistan and Surrounding Countries. In *Transboundary Water Resources in Afghanistan*; Elsevier: Amsterdam, The Netherlands, 2016; pp. 289–309. [CrossRef]
51. Pulkkinen, S.; Nerini, D.; Pérez Hortal, A.A.; Velasco-Forero, C.; Seed, A.; Germann, U.; Foresti, L. Pysteps: An open-source Python library for probabilistic precipitation nowcasting (v1.0). *Geosci. Model Dev.* **2019**, *12*, 4185–4219. [CrossRef]
52. Germann, U.; Zawadzki, I.; Turner, B. Predictability of precipitation from continental radar images. Part IV: Limits to prediction. *J. Atmos. Sci.* **2006**, *63*, 2092–2108. [CrossRef]
53. Atencia, A.; Rigo, T.; Sairouni, A.; Moré, J.; Bech, J.; Vilaclara, E.; Cunillera, J.; Llasat, M.C.; Garrote, L. Improving QPF by blending techniques at the meteorological service of Catalonia. *Nat. Hazards Earth Syst. Sci.* **2010**, *10*, 1443–1455. [CrossRef]
54. Foresti, L.; Reyniers, M.; Seed, A.; Delobbe, L. Development and verification of a real-time stochastic precipitation nowcasting system for urban hydrology in Belgium. *Hydrol. Earth Syst. Sci.* **2016**, *20*, 505–527. [CrossRef]
55. Thorndahl, S.; Einfalt, T.; Willems, P.; Ellerbaek Nielsen, J.; Ten Veldhuis, M.C.; Arnbjerg-Nielsen, K.; Rasmussen, M.R.; Molnar, P. Weather radar rainfall data in urban hydrology. *Hydrol. Earth Syst. Sci.* **2017**, *21*, 1359–1380. [CrossRef]
56. Ayzel, G.; Heistermann, M.; Winterrath, T. Optical flow models as an open benchmark for radar-based precipitation nowcasting (rainymotion v0.1). *Geosci. Model Dev.* **2019**, *12*, 1387–1402. [CrossRef]
57. Raj, B.; Sahoo, S.; Puviarasan, N.; Chandrasekar, V. Operational assessment of high resolution weather radar based precipitation nowcasting system. *Atmosphere* **2024**, *15*, 154. [CrossRef]
58. Hofmann, J.; Schüttrumpf, H. Risk-based and hydrodynamic pluvial flood forecasts in real time. *Water* **2020**, *12*, 1895. [CrossRef]
59. Löwe, R.; Thorndahl, S.; Mikkelsen, P.S.; Rasmussen, M.R.; Madsen, H. Probabilistic online runoff forecasting for urban catchments using inputs from rain gauges as well as statically and dynamically adjusted weather radar. *J. Hydrol.* **2014**, *512*, 397–407. [CrossRef]
60. Fava, M.C.; Mazzoleni, M.; Abe, N.; Mendiondo, E.M.; Solomatine, D.P. Improving flood forecasting using an input correction method in urban models in poorly gauged areas. *Hydrol. Sci. J.* **2020**, *65*, 1096–1111. [CrossRef]
61. Chen, G.; Hou, J.; Zhou, N.; Yang, S.; Tong, Y.; Su, F.; Huang, L.; Bi, X. High-resolution urban flood forecasting by using a coupled atmospheric and hydrodynamic flood model. *Front. Earth Sci.* **2020**, *8*, 545612. [CrossRef]

62. DHI Group. Strengthening Bangkok's Early Warning System to Respond to Climate Induced Flooding. DHI Business Management System Certified by Bureau Veritas to Comply with ISO 9001 (Quality Management). 2017, pp. 1–11. Available online: https://www.ctc-n.org/sites/www.ctc-n.org/files/resources/strengthening_bangkoks_early_warning_system_to_respond_to_climate_induced_flooding.pdf (accessed on 31 March 2024).
63. Hansen, L.S.; Borup, M.; Moller, A.; Mikkelsen, P.S. Flow forecasting using deterministic updating of water levels in distributed hydrodynamic urban drainage models. *Water* **2014**, *6*, 2195–2211. [[CrossRef](#)]

Disclaimer/Publisher's Note: The statements, opinions and data contained in all publications are solely those of the individual author(s) and contributor(s) and not of MDPI and/or the editor(s). MDPI and/or the editor(s) disclaim responsibility for any injury to people or property resulting from any ideas, methods, instructions or products referred to in the content.